1991

Detection and classification of frequency-hopped spread spectrum signals

James Eric Dunn
Iowa State University

INFORMATION TO USERS

This manuscript has been reproduced from the microfilm master. UMI films the text directly from the original or copy submitted. Thus, some thesis and dissertation copies are in typewriter face, while others may be from any type of computer printer.

The quality of this reproduction is dependent upon the quality of the copy submitted. Broken or indistinct print, colored or poor quality illustrations and photographs, print bleedthrough, substandard margins, and improper alignment can adversely affect reproduction.

In the unlikely event that the author did not send UMI a complete manuscript and there are missing pages, these will be noted. Also, if unauthorized copyright material had to be removed, a note will indicate the deletion.

Oversize materials (e.g., maps, drawings, charts) are reproduced by sectioning the original, beginning at the upper left-hand corner and continuing from left to right in equal sections with small overlaps. Each original is also photographed in one exposure and is included in reduced form at the back of the book.

Photographs included in the original manuscript have been reproduced xerographically in this copy. Higher quality 6" x 9" black and white photographic prints are available for any photographs or illustrations appearing in this copy for an additional charge. Contact UMI directly to order.

U·M·I

University Microfilms International
A Bell & Howell Information Company
300 North Zeeb Road, Ann Arbor, MI 48106-1346 USA
313/761-4700 800/521-0600

Order Number 9202348

Detection and classification of frequency-hopped spread spectrum signals

Dunn, James Eric, Ph.D.

Iowa State University, 1991

U·M·I
300 N. Zeeb Rd.
Ann Arbor, MI 48106

Detection and classification of frequency-hopped spread spectrum signals

by

James Eric Dunn

A Dissertation Submitted to the

Graduate Faculty in Partial Fulfillment of the

Requirements for the Degree of

DOCTOR OF PHILOSOPHY

Department: Electrical Engineering and Computer Engineering
Major: Electrical Engineering

Approved:

Signature was redacted for privacy.

In Charge of Major Work

Signature was redacted for privacy.

For the Major Department

Signature was redacted for privacy.

For the Graduate College

Members of the Committee:

Signature was redacted for privacy.

Iowa State University
Ames, Iowa

1991

LIST OF FIGURES

LIST OF TABLES

I. INTRODUCTION

Spread spectrum modulation was developed as a result of the need for secure military communications. Reasons for the development and utilization of spread spectrum modulation are to provide protection against jamming (either accidental or intentional), unauthorized detection, and signal interception [1]. The need for robust communications systems with these attributes became apparent during World War II [2] because of the widespread use of electronic warfare.

The theoretical and technical foundations of modern spread spectrum systems were developed shortly after the war by publication of Shannon's information theorem [3] and the development of practical hardware correlators. One of the first operational frequency-hopped spread spectrum system was BLADES [2], which was developed in the mid-1950's for the navy. Spread spectrum systems employing direct-sequence or time hop modulation were also developed in this time frame. Since the 1950's, the major advances in spread spectrum have been technological improvements to increase the jamming margin and reduce the synchronization time at the receiver.

In the past ten years, the use of spread spectrum communications has become more prevalent, especially in military communications. Major uses of spread spectrum modulation include jam and interception resistant military

communications such as JTIDS (Joint Tactical Information Distribution System) or SINCGARS (Single Channel Ground-Airborne Radio System) [4], provision of accurate location and time information through satellites with GPS (Global Positioning System), experimental communications systems [5], and digital cellular and personal communications networks.

This dissertation proposes a means of defeating Frequency-Hopped (FH) spread spectrum modulation using an intercept receiver capable of fast spectral analyses and emission classifications. The intercept receiver uses fast spectral analyses to detect individual emissions from FH signals, while the classification algorithm is used to match detected emissions with known FH signals. To illustrate the application of the classification algorithm, an example that uses hop frequency order statistics to classify emissions based on the emission frequency and the hopping spans of FH signals is given. No *a priori* knowledge of the FH signals is needed by the classification algorithm or the receiver before emissions can be classified.

Motivation for this research comes from the fact that the primary purpose of FH modulation is to provide secure military communications, and considerable tactical advantage can be gained by rendering the FH communications of one's opponent open to intelligence gathering (detection, eavesdropping, or position location) or electronic warfare (jamming or other

disruption). A side benefit of this research is that it provides the ability to determine the vulnerability of one's own spread spectrum communications to interception or disruption.

The first step in the interception of FH signals is emission detection. Common structures suitable for FH signal detection include radiometers [6]-[15], and compressive receivers [16][17]. Although compressive receivers have begun to receive considerable attention, radiometry remains, by far, the most widely discussed method of signal detection. The popularity of radiometry for emission detection is due both to its ease of implementation in the analog and digital domains, and to an abundance of articles analyzing radiometer behavior.

Current research into the detection of FH signals involve the use of sub-optimal detectors for easier implementation [9][14], combining the outputs of many narrowband detectors to increase the probability of detection [9], and applying the method of Wald to energy detection [13]. A comprehensive study on the effects of changing integration times and detection bandwidths on the probability of detection was conducted by Dillard in [12] and later [7]. An interesting method developed by Gardner [10] calculates the autocorrelation of the Fourier transform of a signal for the detection of both emissions and cyclic features such as the baud and hop rates of a FH signal.

Only a radiometric detector was considered for this dissertation. A summary of the various detection strategies is discussed, and a functional diagram of a digital channelized detector presented. The constraints imposed on the sampling rate and bin width of the digital detector by the hopping span of the FH signal are presented in detail, as well as the relationship of the digital detector to analog radiometers. Finally, a method for reducing the length of a receiver time epoch using parallelism in the receiver architecture is presented.

Correct classification of emissions is the second fundamental problem that must be addressed before signal interception is possible. FH signal interception is complicated by the presence of other signals with both spread spectrum and conventional modulation in the same region of the spectrum as the signal(s) of interest. The interceptor must be able to detect and identify emissions from FH signals despite the potential presence of many other signals with uncertain spectra. With no *a priori* knowledge of the FH signals, the intercept receiver tries to negate the anti-intercept property of signals with FH spread spectrum modulation, and render them vulnerable to disruption or exploitation.

Many articles in the current literature discuss how to calculate data that can be used for emission classification,

or use an ad hoc method to exploit a single feature. For example, automatic modulation recognition from discrete-time samples of an emission [18]-[21] is needed for demodulation of FH signals, and can also be used as data for the classification algorithm. Other examples of suitable data exist ([10] and [22], for example), but the use of such data for emission classification has received less attention.

The classification algorithms developed for this dissertation have the capability of using data with any probability distribution function to classify detected emissions. This compares with ad hoc methods such as [16] which uses only time-of-arrival of emissions, has not been developed into a probabilistic model, and is therefor incapable of incorporating any other data in its classification decisions. A classification algorithm using data with Gaussian distributions has been presented [23], but this algorithm is unable to exploit data which do not have gaussian distributions (emission frequency or time-of-arrival, for example). An example using emission frequency as a aid to emission classification is developed both to demonstrate how to generate probabilistic models for data, and to show how such data can be used along with data with Gaussian distributions to improve classification accuracy.

Digital processing is becoming increasingly feasible for use in receiver design [19][24] due to the development of more

powerful digital processors [25] and extremely linear analog-to-digital (A/D) converters. As digital processors become more powerful and costs fall, more receiver functions can be implemented using digital techniques. In essence, this can be accomplished by moving the A/D converter function from the output toward the antenna until practical technology, performance, and cost limits are reached. The trend in receiver design has been to introduce digital processing in the latter stages of the receiver where the processing requirements are not as severe.

An intercept receiver needs to perform both emission detection and classification to operate successfully in potentially complicated electromagnetic spectrums. An all-digital intercept receiver has an advantage over an analog receiver in that samples used to compute the spectral density (for signal detection) can be easily stored and used again for signal feature estimation and emission classification. More and more articles in the current literature discuss not only the detection of spread spectrum signals, but also the estimation of a signal feature using discrete-time samples of the received signal.

The emission sorting and classification algorithms developed for this dissertation were designed for use with a digital receiver. This was because the level of technology is fast approaching the point where digital radio theory and

techniques are becoming increasingly feasible in cost. This trend is evidenced in current military communication equipment design which is leaning toward digital implementation of as many signal processing functions as practical. The benefits of digital processing (reduced size, power consumption, increased flexibility) can be realized in the portions of the receiver that replace conventional analog circuitry with digital processing. In addition, digital processing allows the application of new techniques to intercept receiver design by implementing functions that can not be duplicated in an analog receiver.

The proposed receiver uses Fast Fourier Transforms (FFT's) of the received signal for emission detection and a Baysian emission classification algorithm. The detection performance of the digital receiver is compared with conventional analog receivers using energy detectors for emission detection. The accuracy of the proposed algorithms is also examined. Because an analog counterpart to the emission classification algorithm does not exist and few articles exist in the open press, no comparisons to existing emission classifiers can be drawn.

II. DEFINITIONS AND TERMINOLOGY

Frequency-hopped modulation was developed as a means of providing secure, low probability of intercept communications by pseudo-randomly changing the carrier frequency of a narrowband signal. Define the unit pulse function $\rho(y)$ to be

$$\rho(y) = \begin{cases} 1 & \text{if } y \in [0,1) \\ 0 & \text{otherwise} \end{cases} \tag{1}$$

Using the unit pulse function, a signal with frequency-hopped (FH) modulation is expressed as

$$s(t) = \sum_{k=-\infty}^{\infty} A(t) \sin\left(2\pi (f_0 + c_k B_c)\, t + \theta(t)\right) \rho\left(\frac{t - k\tau_c}{\tau_c}\right) \tag{2}$$

where k is the dwell index, $\{c_k\}$ is the pseudo-random spreading code, B_c is the channel spacing, $f_0 + c_k B_c$ is the hop frequency and τ_c is the dwell time (the length of time at a hop frequency). The amplitude function, $A(t)$, and the phase function, $\theta(t)$, are determined by the transmitted data and the type of modulation used to produce the non-hopped bandpass signal. The spreading code has positive and negative values, so the hop frequencies are evenly distributed around f_0.

From equation (2), a FH signal is seen to be composed of a sequence of gated fixed-frequency signals, $s_k(t)$, where

$$s_k(t) = A(t)\sin(2\pi(f_0+c_{kB_c})t+\theta(t)) \qquad (3)$$

The k-th signal is multiplied by the pulse function so that it contributes to the FH signal only during the time interval $k\tau_c \le t < (k+1)\tau_c$. Each gated fixed-frequency signal that forms part of the FH signal is called an emission. During the period of time that a single emission is present, known as a *dwell*, the FH signal appears indistinguishable from a fixed frequency signal with the hop frequency equal to the emission frequency. Only over longer intervals of time does the pseudo-random nature of the spread spectrum modulation become apparent. When observed for a period of time equal to several dwells, a FH signal appears as a passband signal that changes carrier frequency or "hops" every τ_c seconds.

The hopping span of a FH signal is defined to be the region of the electromagnetic spectrum that contains all the emissions that comprise the signal. For purposes of definition, let the hopping span be the interval $f_l \le f \le f_h$, where

$$\begin{aligned} f_l &= \min_k \{f_0+c_kB_c\} \\ f_h &= \max_k \{f_0+c_kB_c\} \end{aligned} \qquad (4)$$

The hop bandwidth B_h of a FH signal is defined to be the width of the hopping span, or

$$B_h = f_h - f_l \tag{5}$$

The hop bandwidth is typically large when compared to the bandwidth of the non-hopped signal, since the interference rejection gained through the use of spread spectrum modulation is proportional to the hopping bandwidth.

The number of channels is the total number of hop frequencies that a FH signal can produce. The number of channels is limited by either the transmitter hardware or the pseudo-random spreading code. The number of channels can be calculated from the hop bandwidth and the channel spacing using the relationship

$$N_c = \frac{B_h}{B_c} + 1 \tag{6}$$

Equations (2)-(6) define the features which uniquely identify a FH signal, and can be used to help classify detected emissions. Other signal features such as azimuthal angle-of-arrival and wave polarization are potentially very useful in emission classification, but are not included as part of the definition of a FH signal.

Equation (2) shows that over the period of a dwell, a FH signal is indistinguishable from a fixed frequency signal. Only over periods of time longer than a dwell does the pseudo-random behavior introduced by the spread spectrum modulation

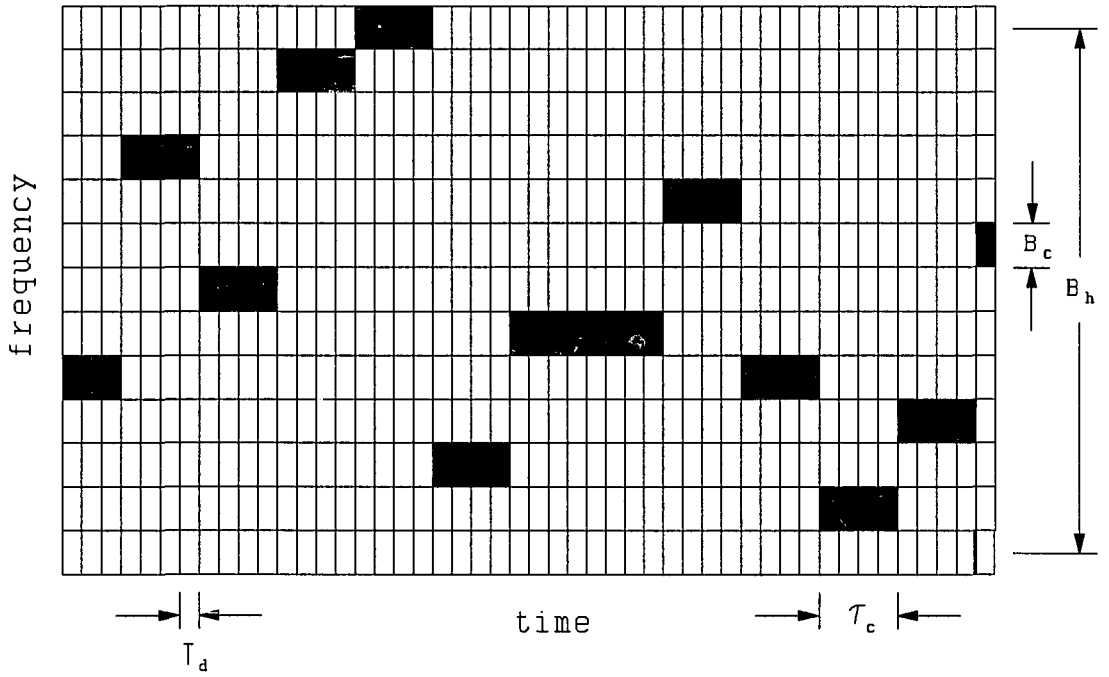

Figure 1. Frequency versus time display showing how a FH signal appears over a period of many dwells

become apparent. The classification algorithm uses this characteristic of FH signals to identify the existence of a FH signal. The classification algorithm uses data calculated from samples of an emission to group emissions with similar features. By continuously analyzing the frequency spectrum and classifying detected emissions, the classification algorithm can be used to follow a FH signal as it "hops" over time.

Figure 1 is a frequency versus time representation of how a FH signal appears to an intercept receiver. The black areas represent occupied regions of the spectrum. Each dwell appears as a black rectangle, occupying a narrow portion of

the spectrum for a period of time. The horizontal axis represents time, and is divided into divisions representing the length between receiver time epochs. A single spectral density estimate is produced and processed by the receiver during an epoch. Receiver time epochs occur at integer multiples of $t=T_d$ seconds. The vertical axis shows the frequency span being analyzed, and is divided into divisions representing the granularity of the spectral density estimates which, in this example, is equal to the emission bandwidth. By inspection, a single FH signal with at least twelve possible hop frequencies and a dwell time of four receiver time epochs is present.

The dwells of the FH signal shown in Figure 1 are precisely aligned with the time epochs in the intercept receiver, although this will not usually be true. If a time misalignment exists, it will introduce an uncertainty of one epoch in the epoch-of-arrival and divide the emission power between frequency bins during any epoch where the FH signal changes hop frequency. If the period between time epochs in the intercept receiver is shorter than the dwell time, misalignment in time is not a serious problem. As an illustration, consider the effects of a misalignment with the FH signal represented in Figure 1. During the first and last epochs an emission is present (in a single frequency bin), the

detection performance is degraded because the emission is not present during the entire epoch. However, there will be three epochs during which the emission is present the entire epoch, and the probability of detection is not degraded.

To provide insight into the difficulty of the task facing an intercept receiver, specifications for some existing FH systems are examined. Existing systems typically have many hops per second since "fast" hopping signals are more difficult to jam. Dixon [4] describes a system called SINCGARS (Single Channel Ground-Airborne Radio System) which has a hopping span of 30-88 MHz, a channel spacing of 25 kHz, and a hopping rate of 25,000 hops per second. A SINCGARS emission will be present in one of more than 2200 channels for only 40 microseconds. To detect these emissions, an enormous amount of data must be processed. This huge volume of information implies that data reduction will be an important factor in a practical intercept receiver. To conserve limited system resources, only those channels that are judged most likely to contain FH emissions can be examined in detail.

A more realistic representation of the electromagnetic spectrum encountered by an intercept receiver is shown in Figure 2. The frequency versus time graph shown is drawn closer to scale because the channel spacing of the FH signals is very small when compared to the total bandwidth analyzed by the receiver. By examining the frequency versus time display,

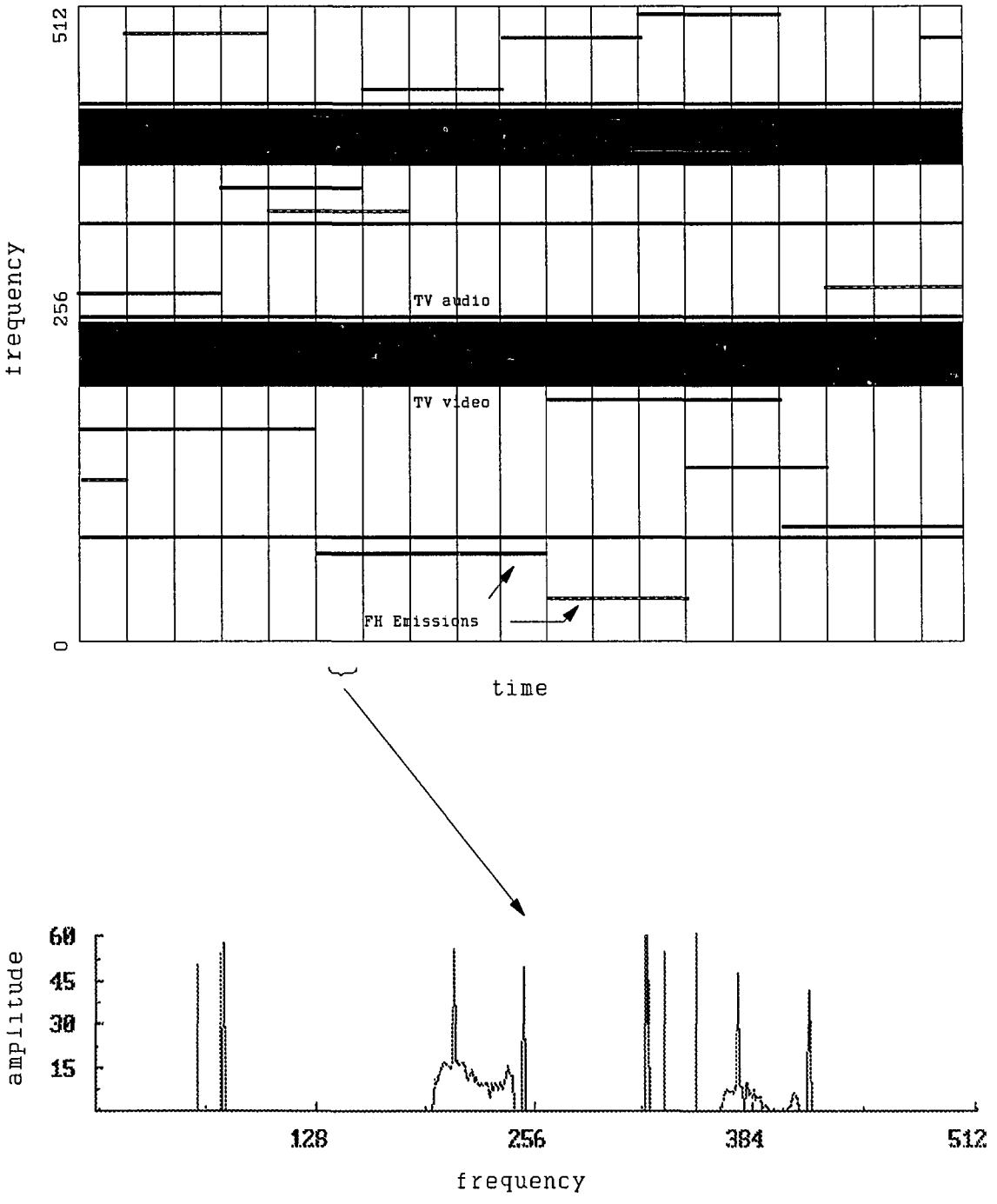

Figure 2. Frequency versus time display drawn to scale (upper portion) and spectral density at the receiver during one epoch (lower portion)

three FH signals, two wideband signals (television signals including the audio carriers), and two fixed frequency narrowband signals are seen.

The FH signals shown in the figure can be uniquely identified by differences in their dwell times, epochs-of-arrival, and hop bandwidth. Examination of the spectral density display shows that the two wideband signals are television signals. Two emissions from the FH signals do not appear in the frequency versus time display. The most likely reason for this is because the emission frequency falls in the region of the spectrum occupied by one of the television signals. An intercept receiver must be able to detect and correctly classify FH emissions in realistic signal environments like that shown in Figure 2.

The large number and variety of signals present in the environment mean that a robust, accurate classification algorithm is needed. The best way to develop an algorithm that meets this criterion is to first obtain a thorough understanding of the theory behind such algorithms. Having defined the form of a FH signal and the parameters that uniquely characterize it, the theoretical basis of the solutions to the detection and classification problems developed for this research are addressed in the following chapter.

III. THEORETICAL BASIS FOR HYPOTHESIS TESTS

In this chapter, the statistical theory that serves as the framework for the signal detection and emission classification algorithms is briefly described. It is important that the theoretical foundations of the algorithms be well understood so the assumptions, strengths, and weaknesses of the techniques are apparent. Both the signal detection and the emission classification algorithms rely heavily on Baysian decision theory, although the specific implementations are common enough to have been named. A general discussion of Baysian decision theory is presented first, followed by specific examples of how this theory is applied to obtain practical emission detection and classification algorithms.

A. States of Nature, Data and Data Distributions

In the most general possible statement about Baysian theory, a decision about the current state of nature must be made based on observed data drawn from some distribution(s). The data distributions are assumed to be dependent on the current state of nature, and the decision problem is how best to identify the state of nature given the observed data.

When the states of nature form a continuous sample space, the decision process is called an estimation problem. From this branch of statistical theory comes estimation algorithms such as maximum likelihood estimators, linear estimators, and method of moments estimators. These techniques are well understood and information about them can be obtained from a variety of sources [26][27], so they are not discussed further here. Of more interest to this dissertation is the situation that exists when the states of nature form a finite or countably infinite set. In this case, the decision process is called a hypothesis test or a decision problem [28].

The signal detection problem is an example of a hypothesis test. The states of nature and possible decisions comprise a set with only two elements: signal present, and signal absent. When an energy detector is used as the source of the observed data, the data have a non-central chi-square distribution when the input to the detector consists of a signal plus noise, and a chi-square distribution when noise is the only input to the detector [6].

The emission classification problem also is an example of a hypothesis test because the states of nature form a finite set. The purpose of the hypothesis test is to identify from which FH signal a detected emission comes. There are thus N_s states of nature, where N_s is the number of known signals. A

practical emission classification algorithm also has to account for the small, but finite, probability that a detected emission is an artifact of noise, or is the first emission from a new, previously inactive signal. The inclusion of these details does not add substantially to the understanding of how to classify detected emissions, so the classification problem considered in the remainder of this dissertation is limited to how to select the best match for an emission from a known number of signals.

To classify a detected emission, the receiver assigns to it a number, j, corresponding to which FH signal the receiver concludes the emission is from. Each decision, $d(x)=j$, is the intercept receiver's best estimate to which FH signal the emission is matched based on the observed data, x. The observed data for the signal classification problem are calculated from samples of detected emissions, and are assumed to consist of estimates of signal features such as the magnitude, or the azimuthal angle-of-arrival. The probability distribution functions of the data are dependent on the method used for data collection, so the classification algorithm must be able to incorporate data with continuous, discrete and degenerate distributions.

B. Loss, Risk, and Bayes Risk

Whether the decision is an estimation problem or a hypothesis test, a function which describes the quality of each possible decision is needed. The quality can be either the "goodness" or the "badness" associated with possible decisions. If the function defines the "goodness" of each decision, the decision rule that maximizes the average value of the function is found. When the function defines the "badness" of each possible decision, the decision rule that minimizes the function is found. This latter approach is more common, and the function which defines the "badness" or "harm" associated with each decision is called the loss function.

The loss function, commonly referred to in engineering as the cost, is an attempt to systematically evaluate the "badness" or "loss" associated with incorrect decisions. The loss function maps the states of nature and possible decisions onto the non-negative real numbers. Its only constraint is that it must be non-negative. The loss function, $L(I,d(x))$, is a function of both the possible states of nature, I, and the decision rule, $d(x)$.

The risk is defined to be the expected value of the loss,

and is calculated using the probability distribution function[1] of the observed data. The notation $E_I[\cdot]$, denoting the expected value conditioned on the random variable, I, is used to express the risk as

$$R(I,d) = E_I[L(I,d(x))] \tag{7}$$

When the probability distribution functions of the observed data are continuous, equation (7) is equivalent to

$$R(I,d) = \int_X L(I,d(x))\, g(x|\phi^I)\, dx \tag{8}$$

The average loss is calculated by multiplying the loss by the probability density function of the data, $g(x|\phi^i)$, and then integrating over all possible values of the data. The distribution parameters, ϕ^i, are needed to characterize the probability distribution of the observed data (for example, the mean and variance of a Gaussian distribution).

In Baysian analysis, the distribution parameters for the states of nature are also assumed to have a distribution, $\pi(\phi)$, called the prior distribution. The Bayes risk, $r(\pi,d)$, is the average risk for all states of nature obtained for a given prior distribution and decision rule, or

---

[1] Probability distribution function (pdf) will be used to refer to a function that can be either continuous or discrete. Probability density function refers to a continuous pdf, while probability mass function refers to a discrete pdf.

$$r(\pi, d) = E_{\pi}[R(i, d)] \tag{9}$$

The Bayes rule, $d_b(x)$, for a prior distribution is that decision rule which minimizes the Bayes risk, or

$$r(\pi, d_b) = \min\{r(\pi, d)\} \tag{10}$$

Different Bayes rules can be obtained by changing the data distribution, loss function, or prior distribution. The probability distribution function of the observed data usually models some physical process, and is not, in general, a quantity that can be easily changed. Alternately, the loss function and prior distribution are parameters which can be altered, and are frequently chosen so the resulting Bayes rule has a simple form.

A loss function which is frequently used for hypothesis testing is zero when a correct decision is made, and one when an incorrect decision is made. The Bayes rule that results from use of this loss function generally has a simple form. When a zero/one loss function is used, the risk is equivalent to the probability of an incorrect decision for a state of nature. The Bayes risk is the average probability of an error (an incorrect decision) for all possible states of nature. Because the Bayes rule minimizes the Bayes risk, it will also minimize the average probability of error when this particular loss function is used.

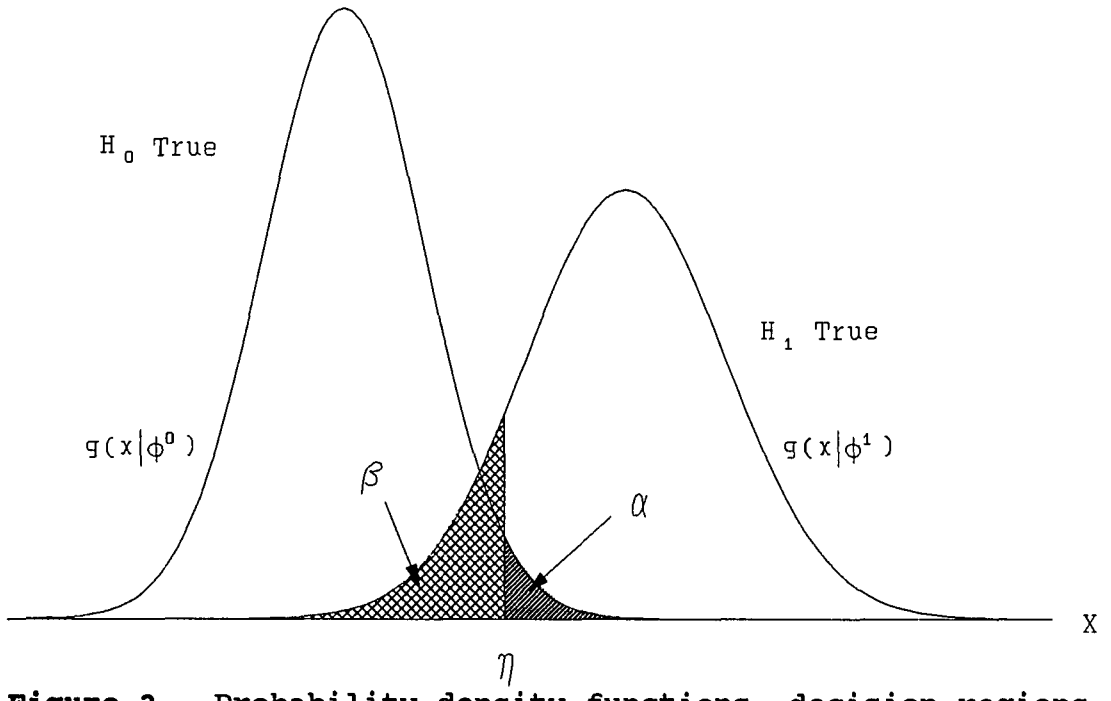

Figure 3. Probability density functions, decision regions, size and power for the signal detection hypothesis test

The signal detection problem, graphically illustrated in Figure 3, is used to illustrate the concepts of data, data distributions, loss, and risk. The two states of nature are signal present (i=1) and signal absent (i=0). The observed data are drawn from one of two different probability distribution functions, $g(x|\phi^0)$ or $g(x|\phi^1)$, depending on the current state of nature.

The hypothesis test is equivalent to a test to determine the probable distribution of the data, or

$$H_0 : X \sim g(x|\phi^0)$$
$$H_1 : X \sim g(x|\phi^1) \qquad (11)$$

where H_0 is the null hypothesis, H_1 is the test hypothesis, ϕ^i is the distribution parameter(s) for each state of nature, and $g(x|\phi^i)$ is the probability density function of the data under the i-th hypothesis.

C. Size and Power of a Hypothesis Test

The size of the hypothesis test is the expected value of the loss under the null hypothesis. When a zero/one loss function is used, the size of the hypothesis test is equal to the probability of erroneously choosing the test hypothesis. In the signal detection problem, the decision rule can be shown to be equivalent to a comparison with a threshold, η. The size of the hypothesis test, represented by α in Figure 3, is more commonly referred to as the probability of false alarm.

The power of the hypothesis test is one minus the expected value of the loss under the test hypothesis. When a zero-one loss function is used, the power is equivalent to the probability of accepting the test hypothesis when the test

hypothesis represents the true state of nature. This is graphically depicted by the quantity $1-\beta$ in Figure 3. In the signal detection problem, the power of the test is more commonly called the probability of detection.

To illustrate these concepts further, the signal detection problem based on a single observation of the output of an energy detector is examined. In this instance, the datum has a chi-square distribution when no signal is present, $g(x|\phi^0)$, and a non-central chi-square distribution, $g(x|\phi^1)$, when a signal is present at the input to the energy detector [6].

Let the signal power, when present, be constant. This assumption corresponds to selecting a degenerate prior distribution. A zero/one loss function is selected as the loss function, and each state of nature is assumed to be equally likely. The loss in this case is given by

$$L(i,d(x)) = \begin{cases} 0 & \text{if } d(x)=i \\ 1 & \text{if } d(x)\neq i \end{cases} \qquad (12)$$

The risk is given by the average value of the loss. When no signal is present the risk equals

$$R(0,d) = 0\cdot P[d(x)=0|i=0] + 1\cdot P[d(x)=1|i=0] \qquad (13)$$

Similarly, the risk when a signal is present is given by

$$R(1,d) = 1 \cdot P[d(x)=0 \mid i=1] + 0 \cdot P[d(x)=1 \mid i=0] \tag{14}$$

Because the prior distributions are degenerate, the Bayes risk is equal to the average of equations (13) and (14), or

$$\begin{aligned} r(\pi,d) = {} & P[I=0] \cdot (0 \cdot P[d(x)=0 \mid i=0] + 1 \cdot P[d(x)=1 \mid i=0]) \\ & + P[I=1] \cdot (1 \cdot P[d(x)=0 \mid i=1] + 0 \cdot P[d(x)=1 \mid i=1]) \end{aligned} \tag{15}$$

The Bayes rule is found by minimizing the Bayes risk. After discarding terms which are equal to zero and noting that $P[I=0]$ and $P[I=1]$ equal one-half because both states of nature are equally likely, the Bayes risk simplifies to

$$r(\pi,d) = \frac{1}{2}(P[d(x)=1 \mid i=0] + P[d(x)=0 \mid i=1]) \tag{16}$$

The Bayes rule minimizes the Bayes risk given by equation (16). In terms of the data, the value of η that minimizes the Bayes risk needs to be determined to find the Bayes rule for the signal detection problem. Let the null hypothesis be chosen in the region $\{x: -\infty < x \leq \eta\}$, and the test hypothesis chosen in the region $\{x: \eta \leq x < \infty\}$. The Bayes risk will then minimize

$$r(\pi,d) = \frac{1}{2}\int_{\eta}^{\infty} g(x|\phi^0)\,dx + \frac{1}{2}\int_{-\infty}^{\eta} g(x|\phi^1)\,dx \tag{17}$$

This function is minimized when η is selected so that $g(\eta|\phi^0) = g(\eta|\phi^1)$ [26]. Thus, the Bayes rule in this instance is

equivalent to the well-known maximum likelihood (ML) criterion which is expressed as

$$g(x|\phi^0) \underset{H_1}{\overset{H_0}{\gtrless}} g(x|\phi^1) \tag{18}$$

Equation (18) is a compact method of describing the decision rule. The null hypothesis is chosen when the probability distribution function under the null hypothesis is larger than the probability distribution function under the test hypothesis when evaluated using the observed data. If the converse is true, the test hypothesis is chosen. This decision rule is obtained only for the specific choices of a degenerate prior distribution (constant and known amplitude signal), zero/one loss function, and equal *a priori* probabilities for the states of nature described above. Different choices for any of these will change the location of the detection threshold.

D. Neyman-Pearson Decision Criterion

The Neyman-Pearson decision criterion is useful when it is desirable to both minimize the size and maximize the power of a hypothesis test simultaneously. Although desirable, quite frequently this can not be done simultaneously. In the signal detection problem discussed above, a threshold of zero

maximizes the power of the test, but also maximizes the size. Larger thresholds reduce not only the size, but also the power of the hypothesis test. Clearly some compromise is needed to arrive at a satisfactory solution.

The Neyman-Pearson criterion maximizes the power of the hypothesis test while constraining the size of the test to be less than or equal to a specified threshold. In the signal detection problem, the Neyman-Pearson decision criterion is equivalent to maximizing the probability of detection (the power) while maintaining the probability of false alarm (the size) at or below some preselected threshold. The Neyman-Pearson criterion will be used in the following chapter to set a threshold for the energy detector(s) used for signal detection.

E. Useful Statistical Relationships

Several useful relationships from statistical theory used in the derivation of the classification algorithms are mentioned here [27]. First, the law of total probability states that if $B_1, B_2, \ldots, B_k$ is a collection of mutually exclusive and exhaustive events, then for any event A,

$$P[A] = \sum_{i=1}^{k} P[A|B_i] P[B_i] \tag{19}$$

Bayes rule (not the function that minimizes the risk although it has the same name) gives an extremely important relationship between random variables,

$$P[B_j|A] = \frac{P[A|B_j]\,P[B_j]}{P[A]} \tag{20}$$

A useful alternate representation of Bayes rule can be obtained by applying the law of total probability (19) to the denominator of equation (20). The resulting relationship is

$$P[B_j|A] = \frac{P[A|B_j]\,P[B_j]}{\sum_{i=1}^{k} P[A|B_i]\,P[B_i]} \tag{21}$$

Extremely powerful detection and classification algorithms can be developed using just these basic statistical relationships and Baysian analysis.

IV. EMISSION DETECTION

Detection is the first task the receiver must perform to intercept a FH signal. A description of several radiometer configurations for the detection FH signals is presented in this chapter, and the Neyman-Pearson criterion is used to develop signal detection algorithms for the radiometer outputs. A functional diagram of a digital detector which uses Fast Fourier Transforms (FFT's) to implement the radiometer function is proposed. The detection performance of the digital receiver is predicted and compared with conventional analog radiometric receivers. Constraints on the time-bandwidth product imposed by the use of FFT's are also examined. Tradeoffs between detection bandwidth and integration time for both analog and discrete-time systems are examined.

The intercept receiver is commonly assumed to have a general idea of the hopping span, the hop bandwidth, B_h, and the channel spacing, B_c, of the existing FH signals. These characteristics of a FH signal can be determined by physical examination of existing FH transmitters. Unknown signal features that may be of interest include the amplitude and phase functions, and the frequency, at any given time, of emissions from a FH signal. There may also be other signal

features of interest such as the azimuthal angle-of-arrival which are not included in the definition of a FH signal. It is important that the receiver be able to detect individual emissions from a FH signal so estimates of signal features can be calculated.

When the signal to noise ratio is small and the modulation structure is uncertain, intercept receivers using energy detection, or *radiometry*, for emission detection are both practical and effective [6][7][9]. The probability of detection is not dependent on the signal structure or data rate, and a single radiometer is relatively inexpensive to build. Radiometric receivers compare the energy contained in a portion of the spectrum during an observation time to a detection threshold. When the energy is above the detection threshold, a signal is declared to be present.

Radiometers used for signal detection belong to one of two broad categories: wideband radiometers that integrate energy over the time and bandwidth of a frequency-hopped (FH) transmission, and multiple narrowband radiometers matched in time and bandwidth to individual emissions from the transmitter.

A. Wideband Radiometer

The first task confronting an intercept receiver is to

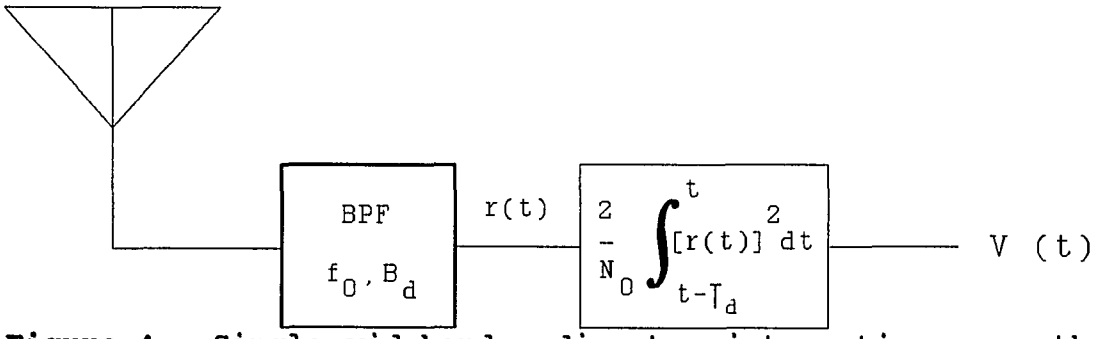

Figure 4. Single wideband radiometer integrating over the entire hopping bandwidth and a time period much greater than a dwell

determine the presence or absence of a FH signal. One of the most basic and effective detectors consists of a single radiometer integrating over the duration and hop bandwidth of a FH signal, as shown in Figure 4. The received signal $r(t)$ is assumed to consist of a frequency-hopped signal, $s(t)$, plus zero-mean, stationary, Gaussian noise, $n(t)$, with flat single-sided power spectral density N_0. The detector consists of a bandpass filter with center frequency f_0 and bandwidth $B_d \geq B_h$. The output of the bandpass filter is squared to produce a signal proportional to the signal (or noise) power, integrated over a period of time $T_d >> \tau_d$, and scaled by the factor $2/N_0$ to normalize the output.

The output, $V(t)$, of the energy detector is closely approximated by a chi-square distribution with $2T_dB_d$ degrees of freedom when the input consists of noise only, and by a non-central chi-square distribution with $2T_dB_d$ degrees of

freedom and noncentrality parameter $\lambda=2E_s/N_0$ when the input consists of a signal with energy E_s plus noise [6]. Signal detection is accomplished by comparing $V(t)$ to the energy detection threshold, η. If $V(t)>\eta$ a signal is assumed to be present. Conversely, when $V(t)\leq\eta$ the input is assumed to consist of noise only. To increase detection performance, the outputs of many separate radiometers are sometimes combined.

In a radiometric receiver, it is not possible to simultaneously minimize the size and maximize the power of the detection algorithm. In addition, the signal strength at the receiver is generally not known in advance, so the receiver cannot be optimized for a single amplitude input signal. Instead, an energy detection threshold is calculated using the Neyman-Pearson criterion so that the radiometer output has a known probability of false alarm (the probability of deciding that a signal is present when the input to the energy detector is noise only).

The energy detection threshold, η, is calculated by solving the expression for the probability of false alarm using the distribution of $V(t)$ when the input consists of noise (the chi-squared distribution). The chi-squared distribution is given by [7]

$$g(v)=\frac{v^{q-1}e^{-v/2}}{2^q\Gamma(q)} \qquad (22)$$

where q is the number of degrees of freedom and $\Gamma(z)$ is the gamma function. When its argument is an integer, the gamma function simplifies to $\Gamma(z)=(z-1)!$.

The size of the hypothesis test, α, is graphically depicted in Figure 3. When applied to signal detection, the size is more frequently called the probability of false alarm, P_{fa}. A probability of false alarm is selected, and the energy detection threshold is calculated by solving the expression for the probability of false alarm

$$P_{fa} = \int_{\eta}^{\infty} \frac{v^{T_d B_d - 1} e^{-v/2}}{2^{T_d B_d} \Gamma(T_d B_d)} dv \qquad (23)$$

The probability of detection is the likelihood of correctly determining the presence of a signal when the input to the detector consists of a signal plus noise. The probability of detection is governed by the noncentral chi-square distribution when the input consists of a sinewave and additive noise, and also closely models the detection performance for modulated sinusoids. The derivation of the probability of detection is discussed in detail in the literature [6][12][7]. To summarize the results, the probability of detection is governed by [7]

$$P_d = \int_{\eta}^{\infty} \frac{1}{2}\left(\frac{v}{\lambda}\right)^{(T_dB_d-1)/2} e^{-(v+\lambda)/2} I_{T_dB_d-1}(\sqrt{v\lambda})\, dv \qquad (24)$$

where $I_\gamma(\cdot)$ is the modified Bessel function of the first kind of order γ, and λ is the signal-to-noise ratio at the energy detector. Equations (23) and (24) define the operating characteristics of an analog radiometric receiver, and will be used as a basis for comparison with signal detection using a periodogram.

A useful approximation that is valid when the time-bandwidth product of the radiometer is large ($T_dB_d \approx 25$ or greater) is that $V(t)$ has a Gaussian distribution with mean $\mu_V = \lambda + 2T_dB_d$ and variance $\sigma_V^2 = 4\lambda + 4T_dB_d$ [7]. This approximation is easily applied to the noise only case by setting $\lambda = 0$ (corresponding to zero signal energy). When this approximation is valid, calculations of the probability of detection can be made from standard tables of the area under the normal curve.

For example, SINCGARS has a hopping span of 30-88 MHz and a channel spacing of 25 kHz. To detect a SINCGARS transmission, a wideband radiometer would analyze a $B_d = 55$ MHz bandwidth. The integration time can be as high as several seconds if signal with extremely low signal-to-noise ratios are of interest [9], because the probability of detection

increases with longer integration times. The period of integration is limited only by the duration of the FH signal, and by the complexities introduced by the time-variant nature of the RF spectrum.

One drawback of the wideband radiometer is that it is only able to determine the presence of a signal, and is unable to determine whether the signal is frequency-hopped. The wideband radiometer is also inherently unable to measure or exploit such signal features as dwell or time-of-arrival of the emissions. The only useful information that can be obtained from a wideband radiometer is thus the mean energy of any signal within the frequency span being analyzed.

Because the wideband radiometer measures the total energy over a large time-bandwidth product, another drawback is that its operation is complicated when multiple signals are present or when the probability distribution function of the noise is not known. The noise may not only be non-white, but also not stationary. A complex signal environment is likely to mask a FH signal, since the energy of the FH signal may be considerably less than the total energy of the other signals present.

B. Channelized Receiver

Channelized receivers are a compromise between

performance and complexity. A channelized receiver analyzes the frequency spectrum using many radiometers, and is useful when the spreading code is of interest, or the signal environment is complex. The channelized receiver shown in

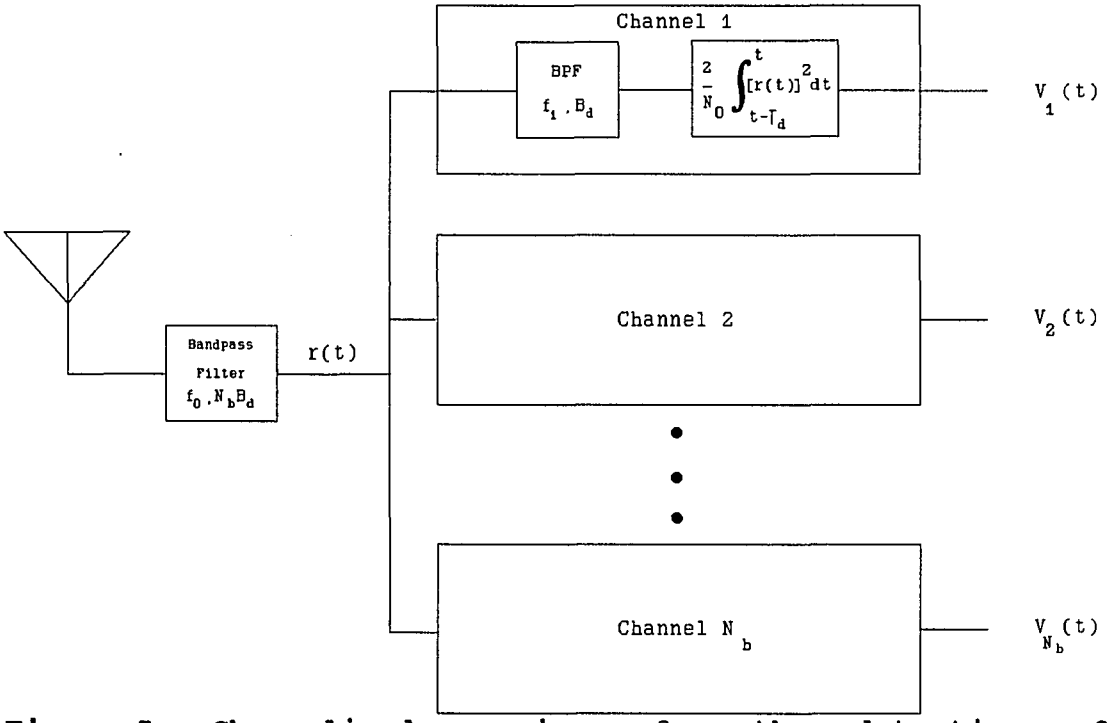

Figure 5. Channelized receiver for the detection of individual emissions from a FH signal

Figure 5 uses N_b radiometers each with bandwidth B_d, where $N_b B_d \geq B_h$, to analyze the hopping span of the FH signal. The channelized receiver is less sensitive to the presence of narrowband fixed-frequency signals because each radiometer is likely to be affected by at most a few fixed frequency emissions, and their effects can be compensated for more easily when they are considered a few at a time. The

integration time of the radiometers in a channelized receiver is less than or equal to the dwell time of the fastest FH signal. This means that the channelized receiver, unlike a receiver which uses a single wideband radiometer for signal detection, can discriminate between a FH signal and a fixed-frequency signal by analyzing the outputs of the energy detectors over time.

When the bin width equals the channel spacing, $N_b=N_c$, and the period of integration equals the dwell time, $T_d=\tau_d$, the channelized receiver is optimized for emission detection (for simplicity, the bandwidth of each emission is assumed to equal the channel spacing). This design has been mainly of academic interest since the large number of hopping channels makes it impractical to build an analog receiver with an energy detector on each hopping channel. To implement an optimum channelized receiver for a SINCGARS transmission, over 2300 energy detectors are required. It would be extremely difficult and costly to implement this number of narrowband filters with the tolerances needed for the energy detectors.

To reduce the number of energy detectors to a more practical level, a common procedure is to set $T_d=\tau_c$ with B_d equal to a multiple of B_c so that each radiometer spans several channels during a dwell. Although no longer optimal, this design represents a reasonable compromise between

detection performance and receiver complexity.

An analog implementation of the channelized receiver shown in Figure 5 requires many narrowband analog filters for the radiometers, and cannot be reconfigured for FH signals with different hop bandwidths or dwell times. Some of these problems can be avoided by replacing the analog radiometers with digital processing. A digital channelized receiver does not need multiple narrowband analog filters, and can be easily reconfigured for different FH signals by changing the sampling frequency and the number of samples used in the spectral density estimate.

C. Digital Channelized Receiver

A block diagram of a direct-conversion receiver with digital baseband is shown in Figure 6. The received signal is prefiltered to avoid aliasing, frequency shifted into the baseband to minimize the sampling rate, and then sampled. After sampling, emissions are detected using a periodogram of the data. Estimates of signal features are calculated for each emission detected by the periodogram. A small delay is added to the sampled data before signal feature estimation to compensate for the time required to calculate the periodogram. This ensures that the same emission detected by the periodogram is available to the signal feature estimator.

Finally, the signal feature estimates are used to classify each detected emission.

Only the effects of the discrete-time analysis are considered here. The effects of amplitude quantization introduced by analog-to-digital converters on detection performance and subsequent processing are not addressed. Each sample of the received signal is assumed to have infinite amplitude resolution. The effects of finite amplitude resolution are frequently modeled as an additive noise source [29], and are not considered here.

The observation time, Δ, is the time required to collect samples for the periodogram. Subsequent processing of the samples is assumed to take less time, so the observation time is the factor which determines the length of time between epochs. At each receiver epoch, detected emissions from the previous epoch are processed while new samples are collected and prepared for processing. The exact samples used to produce the spectral analysis are available for secondary processing by adding digital delay. A data vector is calculated from samples of each detected emission. The data vector is passed to the classification algorithm which identifies which signal produced the emission.

The received signal is first bandlimited to avoid alias distortion after sampling. The detection bandwidth, $N_b B_d$, and

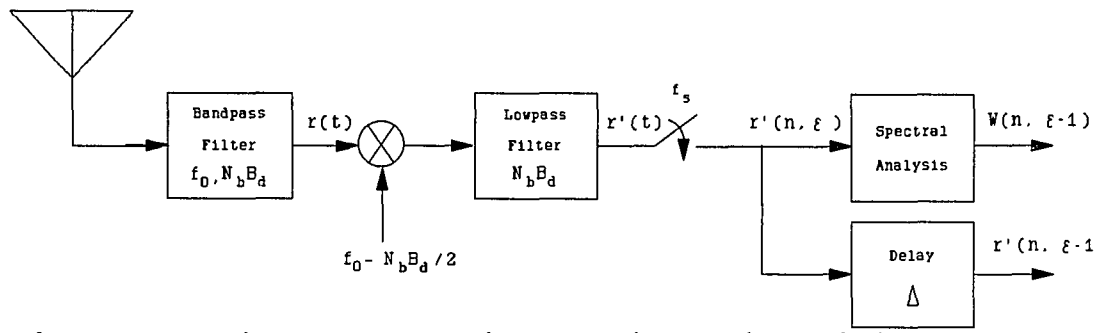

Figure 6. Direct-conversion receiver with digital baseband for the detection of emissions from FH signals

center frequency, f_0, of the receiver prefilter are determined by the hop bandwidth and hopping span of the FH signal. The band-limited signal is then frequency shifted into the baseband and sampled. To avoid aliasing, the sampling frequency must be greater than or equal to twice the prefilter bandwidth, or $f_s \geq 2N_bB_d$.

To produce an N_b bin spectral analysis using a DFT, $N=2N_b$ samples of the input waveform $r'(t)$ are obtained by sampling the input at the sampling rate. During the ϵ-th receiver time epoch, which uses data collected in the time interval $\epsilon\Delta \leq t < (\epsilon+1)\Delta$, the discrete Fourier transform of the samples is calculated using the relationship

$$R'(n,\epsilon) = \sum_{n=0}^{N-1} r'(\epsilon\Delta + n\tau_s)\, e^{-j2\pi nk/N} \qquad (25)$$

where $r'(t)$ is the baseband, frequency-shifted equivalent of $r(t)$. There is a simple one-to-one correspondence between

signals in the original and frequency-translated spectrums given by $R'(f)=R(f+f_0-B_h/2)$, where $R(f)$ and $R'(f)$ are the continuous-time Fourier transforms of $r(t)$ and $r'(t)$ respectively.

The DFT calculates the Fourier transform of the samples at discrete frequencies given by

$$f'_n = \frac{nf_s}{N} \qquad n=0,\ldots,N-1 \tag{26}$$

which directly correspond to the discrete frequencies $f_n=f'_n+f_0-B_h/2$ in the original untranslated spectrum. The FFT produces a double-sided estimate of the spectral density. Positive frequencies correspond to values of n from $n=1$ to $n=N/2-1$, negative frequencies to the range $N/2+1 \le n \le N-1$, while the value associated with $n=N/2$ corresponds to both $f=f_s/2$ and $f=-f_s/2$. The spectral density estimates at corresponding positive and negative frequencies are complex conjugates since the samples were taken from a real-valued function.

This analysis assumes that the samples used to calculate the DFT are taken during a period of time less than a dwell, and that the FH signal hops only at a receiver epoch. Using these assumptions, the spectrum for an epoch will show a narrowband signal in noise. Spectral density estimates, frequently called periodograms, are calculated from the

Fourier transform using the relationship

$$W(n,\epsilon) = \frac{1}{N}|R'(n,\epsilon)|^2 \qquad (27)$$

Both the bin width and the observation time are proportional to the number of samples used in the DFT. As the number of samples increases, the bin width decreases and the observation time increases. Larger periodograms also increase the amount of processing power needed to compute the DFT, increase the amount of high-speed delay needed, and reduce the ability of the detector to identify fast hoppers. For the periodogram to have a bin width equal to the channel spacing of the FH signal, a large number of samples need to be collected. The observation time could potentially be much longer than the dwell time, so the receiver would detect multiple emissions from a single FH signal at each epoch. Thus, practical concerns seem to indicate that both the channelized radiometer and the DFT-based detector must have a bin width larger than the channel spacing of the FH signal, but for different reasons.

A major difference between the DFT-based detector of Figure 6 and the analog channelized radiometric detector of Figure 5 is that T_d is a function of the detector binwidth and cannot be chosen arbitrarily. To show this, first note that the period of integration in the DFT-based detector is equal

to the sampling period multiplied by the number of samples used in the DFT, or $T_d=N/f_s$. The minimum sampling frequency required to satisfy Nyquist's criterion and avoid aliasing is $f_s=2N_bB_d$, or twice the total bandwidth being analyzed. Since $N=2N_b$, the period of integration is seen to be the inverse of the detector binwidth. Since $T_d=1/B_d$ when a single DFT is used for spectral analysis, the time bandwidth product for each bin is unity.

If additional delay in the receiver is acceptable, the time granularity of the receiver can be decreased without a corresponding increase in the bin width. This feat is accomplished using a parallel implementation of DFT's as shown in Figure 7. The parallel implementation trades receiver complexity and delay for additional epochs.

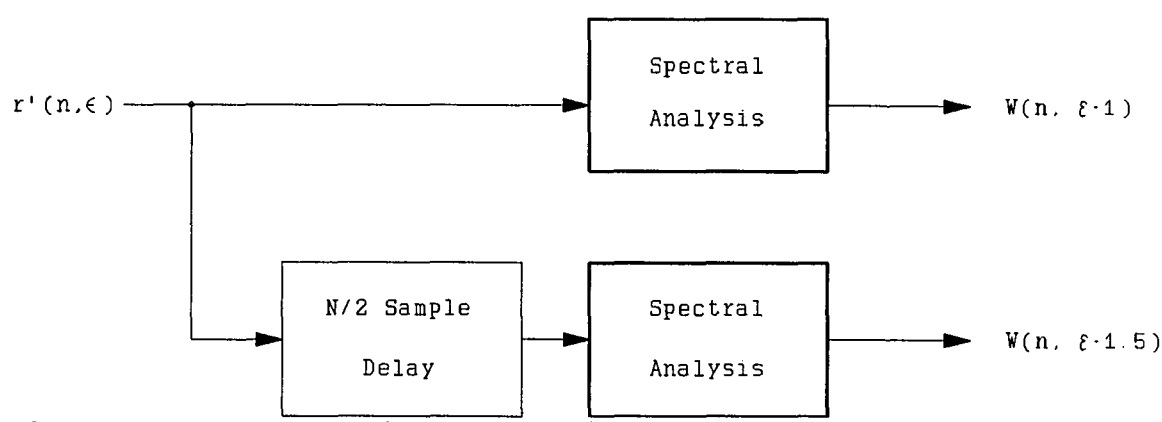

Figure 7. Parallel implementation of DFT's used to decrease the time granularity

In this example, two DFT's of the input sequence are

calculated. The first DFT uses as input the incoming sequence delayed by half the number of samples in the DFT. The second DFT uses the incoming sequence as input. The net effect is that during the observation time, two estimates of the spectral density at two different times are produced. Adding more fractional delay and calculating more DFT's will increase the time resolution of the analyzer proportionally without affecting the frequency resolution. The number of stages can be increased until a DFT is calculated with each sample taken.

The distribution of the spectral density estimates given by equation (27) needs to be determined for comparison with the channelized receiver. To calculate an energy detection threshold for the periodogram, the distribution of $W(n,\epsilon)$ needs to be determined for the noise only case so the Neyman-Pearson criterion can be used.

Let the variance of $r'(t)$ due to noise be denoted by $\sigma_n^2=N_0B_h$. An accurate approximation to the distribution of the periodogram in this case [29][30] is that the quantity

$$\frac{2W(n,\epsilon)}{\sigma_n^2} \tag{28}$$

is chi-square distributed with 2 degrees of freedom. Remember that the output of an analog energy detector also has a chi-square distribution in the noise only case. The distribution

of the normalized samples from the periodogram given by equation (28) is thus identical to the distribution of $V(t)$ from an analog energy detector with a unity time-bandwidth product.

When $T_d B_d=1$ is substituted into equation (23), the resulting equation becomes

$$P_{fa}=\int_{\frac{2\eta}{\sigma_n^2}}^{\infty}\frac{e^{-v/2}}{2}dv \qquad (29)$$

The lower limit of this equation, $2\eta/\sigma_n^2$, is the detection threshold for a normalized periodogram given by (28). The above integral is readily evaluated as

$$P_{fa}=e^{-\eta/\sigma_n^2} \qquad (30)$$

Note from the above expression that the probability of false alarm is dependent only on the variance of the samples and not on the number of samples used in the DFT, so the DFT is not a consistent estimator. Increasing the number of samples used in the DFT will not decrease the probability of false alarm.

By taking the natural logarithm of both sides of equation (30) , the decision threshold for a periodogram is found to be

$$\eta = -\sigma_n^2 \ln P_{fa} \tag{31}$$

To arrive at an upper bound for the probability of detection, several simplifying assumptions are necessary. A first approximation is that each estimate $W(n,\epsilon)$ from the periodogram is equal to the energy contained only in the frequency span $(n-1/2)/N\tau_s \leq f' < (n+1/2)/N\tau_s$ during the epoch. Using this assumption, $W(n,\epsilon)$ can be thought of as an estimate of the energy contained in a frequency bin equal in width to the spacing of the discrete frequencies of the DFT. This assumption is reasonable for a narrowband emission centered on one of the discrete frequencies of the DFT given by equation (26). The periodogram should then have approximately a non-central chi-square distribution with 2 degrees of freedom.

If the emission frequency is not equal to one of the discrete frequencies of the FFT or is not sufficiently narrowband, bin spreading will occur. Bin spreading causes the signal power to be distributed across several frequency bins, and degrades the detection performance of the receiver. Estimates of the probability of detection using the above assumptions therefore represent an upper bound.

A useful approximation to the probability of detection can be obtained by considering an equivalent spectrum that has been created by passing white noise through a shaping filter. The spectral density of a signal plus noise can be

approximated by shaping white noise with a linear filter with gain $|Y(n)|^2=E_s(n)/\sigma_n^2$, where $E_s(n)$ is the signal energy in the n-th bin. From linear systems theory, the spectral density of the noise after shaping by the linear filter will be changed by a factor of $|Y(n)|^2$. The shaped spectrum should also have a chi-square distribution.

The probability of detection using this approximation is given by the probability that the shaped spectrum, $W_s(n,\epsilon)$, is larger than η, or

$$P_d=P[W_s(n,\epsilon)>\eta] \tag{32}$$

To arrive at an expression for the probability of detection, both sides of the argument of equation (32) are scaled to create the expression

$$P_d=P\left[\frac{2W_s(n,\epsilon)}{|Y(n)|^2\sigma_n^2}>\frac{2\eta}{|Y(n)|^2\sigma_n^2}\right] \tag{33}$$

Since $W_s(n,\epsilon)=|Y(n)|^2W(n,\epsilon)$ and $2W(n,\epsilon)/\sigma_n^2$ is approximately chi-square distributed with two degrees of freedom, the quantity $2W_s(n,\epsilon)/|Y(n)|^2\sigma_n^2$ should also have a chi-square distribution with 2 degrees of freedom. By substitution, the probability of detection is equivalent to

$$P_d = P\left[\chi^2(2) > \frac{2\eta}{E_s(n)}\right] \tag{34}$$

where $\chi^2(2)$ represents a chi-square random variable with two degrees of freedom, and $E_s(n) = |Y(n,\epsilon)|^2\sigma_n^2$. Equation (34) is easily evaluated using the chi-square distribution, and is equal to

$$P_d = e^{-\eta/E_s(n)} \tag{35}$$

The variance of the periodogram using the chi-square approximation is proportional to the square of the desired spectrum. The chi-square approximation is useful because of the simplicity of the resulting expression for the probability of detection. It can be used to quickly calculate the approximate probability of detection without having to evaluate the non-central chi-square distribution. As will be shown in Figure 8, this approximation is quite reasonable for signal-to-noise ratios greater than 0 decibels.

A Monte-Carlo simulation was created to examine how accurately the non-central chi-square distribution and the chi-square distribution model the detection performance obtained from a DFT. The simulated signal environment consisted of eight sinusoids with uniformly increasing

amplitudes and random phases in zero-mean unity-variance (σ_n^2=1) Gaussian noise. An N=512 point DFT [31] was used to analyze the signal environment with $P_{fa}=10^{-5}$, a probability of false alarm sufficiently small to ensure that few system resources are utilized analyzing spurious signals. The energy detection threshold was calculated using equation (31). The program DETECT.FOR, included in this dissertation as Appendix A, was created to experimentally determine the probability of detection. The probability of detection predicted by the non-central chi-square distribution was calculated using NCENT.FOR, which is listed in Appendix B. Finally, the probability of detection predicted by the chi-square approximation was calculated using equation (35) and a computer spreadsheet.

Figure 8 is a graph of the data obtained using DETECT.FOR, NCENT.FOR, and the computer spreadsheet. The non-central chi-square distribution models the experimental probability of detection most closely, but equation (35) is also useful at high signal-to-noise rations due to its simplicity.

The fact that the amplitude estimates produced by the periodogram have chi-square distributions when only noise is present suggests a way to improve the detection performance of the receiver. Since the sum of independent chi-square

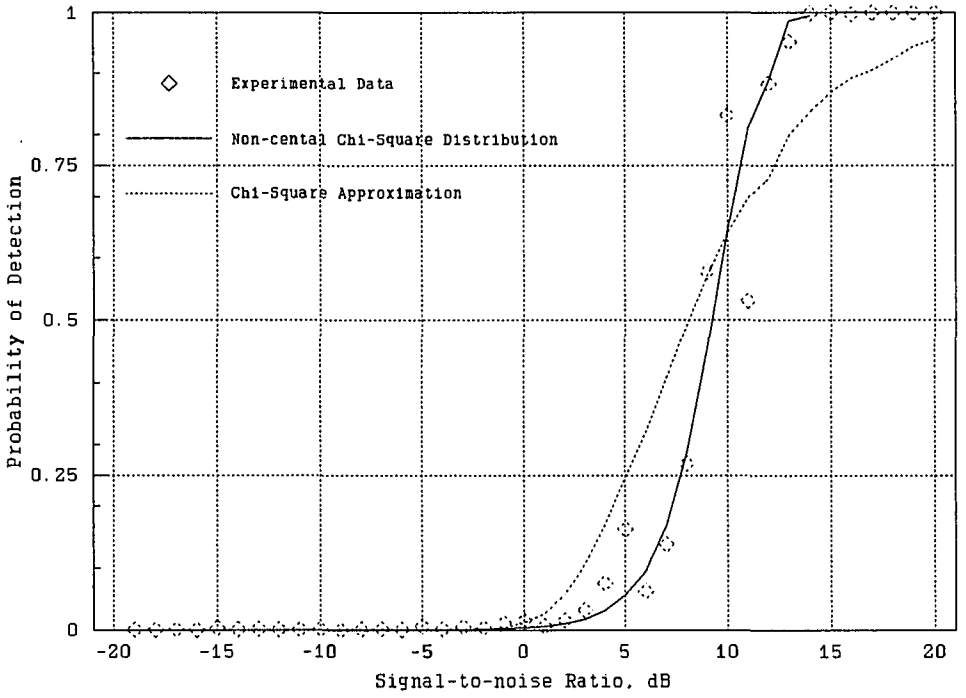

Figure 8. Experimental probability of detection for the periodogram plotted versus the non-central chi-square distribution and the chi-square distribution with 2 degrees of freedom

variables also has a chi-square distribution, N_p successive periodograms can be added together to form an estimate that is also chi-square distributed with $2N_p$ degrees of freedom. The application of this to spectral estimation is frequently referred to as Bartlett's procedure, and it reduces the variance of the periodogram by a factor of N_p [29].

The detection performance of the receiver is important because a compromise between detection performance and the false alarm rate must be reached. If the probability of false

alarm is too low, a large amount of processing power will be wasted analyzing bins that do not contain signals. Conversely, fewer emissions from a FH signal will be observed if the probability of false alarm is set too high, because the probability of detection will be reduced. When fewer emissions are observed, it is harder for the receiver to determine the number of FH signals present.

The decisions as to what level of false alarm is acceptable and what minimum probability of detection is required before the receiver begins to track a signal can only be talked about in generalities, since these decisions are determined primarily by economics. If a low level of false alarm is desirable and a large majority of emissions must be detected, the minimum signal-to-noise ratio is on the order of 10 decibels. Signal interception of the type proposed here is not for signals employing spread spectrum modulation to provide low probability of intercept communications. These signals also will frequently use low data rates and power to make detection difficult. The method of signal interception proposed here would best apply to signals employing FH modulation primarily for jam resistant communications.

V. EMISSION CLASSIFICATION ALGORITHM

While knowledge that a FH signal is present can be important information by itself, exploitation usually requires that some signal feature or features be calculated by the receiver. In this dissertation, interception refers to both the detection and correct classification of the emissions that comprise a FH signal. In this chapter, a maximum likelihood classification algorithm capable of making decisions based on data with discrete, continuous, and degenerate probability distribution functions is developed. This task is complicated by the presence of other signals within the hopping span that may have spread spectrum or conventional modulation. The classification algorithm matches emissions with FH signals by calculating data from emissions (azimuthal angle-of-arrival, as an example) and finding the FH signal most likely to have produced the emission.

Each signal feature describes some aspect of the FH signal that sets it apart from other signals. When the signal environment consists of a single FH signal, signal features can be used by the receiver to identify FH emissions in the presence of spurious emissions. In a more complex environment, use of signal features allows the receiver to identify emissions from a single FH signal in the presence of fixed frequency or even other FH signals.

To ensure accurate classifications under a wide variety of conditions, the receiver should be capable of producing high-quality data dependent on many different signal features. However, cost and computational constraints dictate that only a limited number of data be calculated. As a compromise, the classification algorithm should be flexible enough to exploit all readily available information about a FH signal regardless of the data quality or the form of its probability distribution function. For example, if azimuthal angle-of-arrival and modulation type are the data calculated by the receiver, the classification algorithm makes decisions using data with both continuous (angle-of-arrival) and discrete (modulation type) distributions.

This dissertation considers how emission classifications should be made based on data from dissimilar probability functions using Baysian decision theory. Each datum used by the classification algorithm consists of an estimate of a signal characteristic such as the signal amplitude, and is calculated from samples of a detected emission. Each datum used by the classification algorithm is assumed to be a single sample from a random process with a known probability distribution function. Data calculated from different emissions from the same FH signal should therefore be similar, but not identical.

At each epoch, the receiver first calculates data for the

classification algorithm from samples of each detected emission. Next, the data are used by the classification algorithm to match each detected emission with a known FH signal by finding the signal with the features that most likely produced the data. Classification errors occur when FH signals have similar or nearly identical features. As the number of features estimated by the receiver, N_f, increases, classification errors become less frequent.

Having defined the signal environment for all time in the previous chapter, the epoch dependency of the periodogram and the data will be suppressed for the discussion of the sorting algorithms. This is done both to make an already cumbersome notation more manageable, and because only a memoryless sorter is considered--emission classifications are not dependent on data from previous epochs. To continue to explicitly show the epoch dependency is needlessly confusing.

A. Signal Environment and Terminology

The signal environment for the classification algorithm is assumed to consist of N_s FH signals in additive white Gaussian noise. Because multiple FH signals exist, a method of distinguishing between emissions and parameters from different FH signals is needed. Let the superscript "i" used

with the quantities defined by equations (2)-(6) identify parameters and emissions from the i-th FH signal. For example, B_h^i denotes the hop bandwidth of the i-th FH signal.

Using this notation, the received signal at the prefilter output, $r(t)$, is given by

$$r(t) = n(t) + \sum_{i=1}^{N_s} s^i(t) \tag{36}$$

The observation time of the receiver is assumed to be less than the smallest dwell time of all the FH signals, and FH signals are assumed to hop only at receiver time epochs. The requirement that signals hop only at receiver time epochs allows a discussion of the classification algorithm without addressing effects created when the emission is not present in a bin for the entire epoch. The effects of time misalignment can be minimized by postponing decisions for an epoch or through the use of receiver structures like that shown in Figure 7.

Using these assumptions, each spectral density estimate should show N_s narrowband signals in noise. The classification algorithm presented here does not attempt to determine the dwell index, k, associated with each emission or estimate the hop sequence. Instead, the classification problem determines how to estimate the signal index, i, for

each detected emission.

Let the receiver be capable of estimating N_f signal features, and $\underline{x}=[x_1, x_2, \ldots, x_{N_f}]'$ be a vector of data calculated from samples of a detected emission. Each element x_m of the data vector, $\underline{x}$, is modeled as a sample from a random process with known probability distribution function $g(x_m|\phi_m^i)$, where ϕ_m^i is the distribution parameter for the m-th data probability distribution function from the i-th FH signal. The distribution parameter vector, $\underline{\Phi}^i=[\phi_1^i, \phi_2^i, \ldots, \phi_{N_f}^i]'$, contains all the parameters needed for the probability functions of the data.

The elements of $\underline{x}$ are assumed to be independent random samples from distributions which are parameterized by different signal features. The probability of obtaining the data vector, $\underline{x}$, from samples of an emission from the i-th signal is given by

$$P[\underline{x}|\underline{\Phi}^i]=\prod_{m=1}^{N_f} g(x_m|\phi_m^i) \qquad (37)$$

Two classification algorithms using Baysian decision theory were created for this research. The classification algorithms differ only in their cost functions. The first

algorithm developed is the maximum likelihood emission classification algorithm. In an attempt to correct deficiencies in the maximum likelihood classification algorithm, the epoch classification algorithm was developed.

B. Maximum Likelihood Emission Classification

The well-known maximum likelihood decision criterion [26] is to choose the value of j for each emission that maximizes $P[\underline{x}|\underline{\Phi}^j]$. This algorithm is well-understood and frequently used for hypothesis testing; however, the assumptions used in its derivation are not generally known. The Baysian decision theory on which it is based was discussed in chapter III, and demonstrated with the derivation of a maximum likelihood emission detection algorithm. The assumptions behind the maximum likelihood algorithm are now reviewed.

The first step in deriving a maximum likelihood emission classification algorithm is to assume all the prior distributions are degenerate. This implies the signal features for each observation are constant and known. The loss function, a measure of the harm created by incorrect decisions, is zero for correct decisions and one for incorrect decisions. A final assumption is that the *a priori* probabilities of all of the decisions are equal. Under these

assumptions, the Bayes risk is equal to the probability of an incorrect emission classification.

The maximum likelihood algorithm minimizes the probability of making an incorrect emission classification when all classification errors are considered to have equal weight and all decisions are equally likely [26]. The procedure for classifying FH emissions using the maximum likelihood criterion is thus 1) from samples of each detected emission, $W(n,\epsilon)>\eta$, calculate the data vector, $\underline{x}$, 2) use equation (37) and the probability distribution function for each datum to calculate $P[\underline{x}|\underline{\Phi}^i]$, 3) assign the emission to the j-th signal, where $P[\underline{x}|\underline{\Phi}^j] \geq P[\underline{x}|\underline{\Phi}^i]$ for all $i=1,2,\ldots,N_s$.

When the data have similar probability functions, the classification process can be simplified by using sufficient statistics [27]. As an example, assume the data have independent Gaussian distributions with mean μ_m^i and standard deviation σ_m^i. Equation (37) is given by

$$P[\underline{x}|\underline{\Phi}^i] = (2\pi)^{-N_f/2}\left(\prod_{m=1}^{N_f}\sigma_m^i\right)^{-1} e^{-\frac{1}{2}\sum_{m=1}^{N_f}\left(\frac{x_m-\mu_m^i}{\sigma_m^i}\right)^2} \qquad (38)$$

Simplification of the classification algorithm comes from observing that a necessary and sufficient condition for $P[\underline{x}|\underline{\Phi}^j] \geq P[\underline{x}|\underline{\Phi}^i]$ to occur is that $Q^j \leq Q^i$, where Q^i is the

sufficient statistic for data with independent Gaussian distributions. The sufficient statistic has the form

$$Q^i = \sum_{m=1}^{N_f} \left(\frac{x_m - \mu_m^i}{\sigma_m^i} \right)^2 \qquad (39)$$

Considerable reduction in the computational burden can be achieved through the use of sufficient statistics. Repeated evaluations of the exponential function were avoided in the above example because the sufficient statistics can be compared directly. Equation (39) together with the maximum likelihood algorithm has been proposed as a method of classifying emissions from FH signals by Nicholson, et. al [23]. While their article restricts itself to only data with Gaussian distributions, this analysis is true for any probability distribution function. If the data are not all from the same family of distributions, equation (37) can not be simplified and it is not possible to simplify the test statistics.

The probability of a classification error from maximum likelihood emission classification is tedious to evaluate when many signals are present, especially when the data have different distributions or there are many FH signals present. Let i denote the current state of nature which, in the classification problem, is the FH signal that produced a

detected emission. The probability of classification error is

$$P_e = P[d(x) \neq i] \tag{40}$$

This probability of error is bounded by

$$P_e \leq \sum_{\substack{j=1 \\ j \neq i}}^{N_s} P[P[x|\Phi^i] < P[x|\Phi^j]] \tag{41}$$

Equation (41) is an upperbound for the probability of error because it does not account for the possibility that more than one incorrect signal may be indicated by the algorithm. If the principal source of error is the presence of two FH signals with similar parameters, equation (41) will provide a good approximation to the probability of error. When three or more FH signals have similar features, the approximation will not be as good.

To provide insight into the strengths and weaknesses of the maximum likelihood emission classification algorithm, an example of how the maximum likelihood algorithm can be used to classify emissions using emission frequency is discussed. The example includes the case of both known and unknown signal features, and a discussion on the classification accuracy that can be expected.

C. Classification Using Emission Frequency

In this section, the algorithm created for classifying emissions using emission frequency is described. When hopping spans are known or can be estimated, the emission frequency becomes a valuable source of information for the classification problem. When the hopping spans do not overlap, the emission frequency can, by itself, identify which FH signal produced an emission. When the hopping spans partially overlap, the emission frequency can still be used for emission classification, but the probability of classification error increases.

This derivation will be used both to show how to exploit a fundamental characteristic of FH signals and to demonstrate how signal features with non-Gaussian probability functions can be used for emission classification. As will be seen, in regions where hopping spans overlap, the classification algorithm is equivalent to choosing the FH signal with the smallest hop bandwidth as a match with a detected emission. When hopping spans can be estimated or are known, this knowledge can be used to aid in classifying emissions. To illustrate this concept, both analytical and qualitative arguments are used.

To conform with the requirements for Baysian analysis, the frequency-based classification algorithm assumes that each

hop frequency from the i-th FH signal is a random sample (from the perspective of the receiver) taken from a process with probability mass function $g(f|\phi^i)$. Since the hop frequencies from a FH signal form a discrete pseudo-random sequence and the total number of hop frequencies is usually large, the assumption of a continuous distribution can be used to simplify the calculations. This assumption introduces errors that are small when the bandwidth of the unhopped signal is much smaller than the detector bandwidth.

1. Emission classification with known hopping spans

Consider, first, the trivial case of a signal space which consists of N_s FH signals with precisely known, non-overlapping hopping spans. For these conditions, emissions can be classified without error using only the emission frequency. When an emission is observed, it is matched to the FH signal with the hopping span that contains the emission.

In this example, the data, $X(n)$, used by the classification algorithm is a random variable indicating the spectral occupancy of a portion of the spectrum. The data are a function of both time and frequency, but to avoid needless complexity, the epoch dependency of the data will be suppressed. Define the indicator function $\zeta(\cdot)$ [27] to be

equal to one when its argument is true and zero when it is false. In terms of the indicator function and the periodogram defined in equation (27), the data are expressed as

$$X(n) = \zeta(W(n) > \eta) \tag{42}$$

If the epoch dependency of the data were explicitly shown, the expression for the data would be

$$X(n, \epsilon) = \zeta(W(n, \epsilon) > \eta) \tag{43}$$

Figure 9 shows a simulated periodogram and the data used by the classification algorithm. The periodogram contains three frequency bins with amplitudes greater than the threshold, possibly indicating three signals with different amplitudes. The data used by the classification algorithm as input, $x(n)$, are zero for all but the three frequency bins where $W(n) > \eta$. In those bins, the data are equal to one.

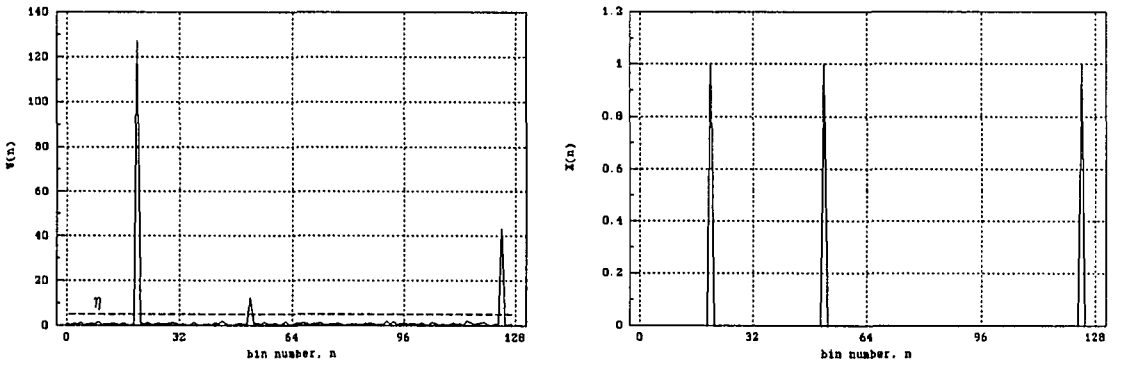

Figure 9. Periodogram and data for emission classification using emission frequency taken from a single epoch

The classification algorithm considers only those

frequency bins where $x(n)=1$, since unoccupied bins are of little interest to the intercept receiver.

Let $g(f_n|\phi^i)$ be the probability that the hop frequency from the i-th FH signal is in the n-th frequency bin during the current epoch. The hop frequencies from each FH signal are assumed to have a discrete uniform random distribution because the spreading code is a pseudo-random sequence and the length of the spreading code is very long compared to any practical observation time. No periodicity can be detected by a practical intercept receiver, so the assumption of a random distribution is justified. The uniform assumption is justified by noting that this distribution is optimum for providing the greatest protection against interference or interception by an unauthorized receiver. Non-uniform distributions are possible, but are sub-optimal.

The probability of occupancy of the n-th bin in the detector by the i-th FH signal is the same as the probability that any hop frequency contained within the bandwidth of the bin will be occupied by an emission. This probability is given by the ratio of 1) the number of hop frequencies contained in each bin of the receiver to 2) the total number of hopping channels, or

$$g(f_n|\phi^i)=\begin{cases}\dfrac{B_d/B_c^i}{N_c^i} & f_l^i \le f_n \le f_h^i \\ 0 & \text{Otherwise}\end{cases} \tag{44}$$

The distribution parameters needed to describe the distribution of hop frequencies is the set $\phi^i=\{f_l^i, f_h^i, B_c^i\}$. The number of hopping channels, N_c^i, is not a necessary parameter because it can be calculated from the other parameters using equation (6). When the number of channels is large, $N_c^i \approx B_h^i/B_c^i$, and equation (44) becomes

$$g(f_n|\phi^i)=\begin{cases}\dfrac{B_d}{B_h^i} & f_l^i \le f_n \le f_h^i \\ 0 & \text{Otherwise}\end{cases} \tag{45}$$

Equation (45) is not a function of B_c^i or N_c^i, so the distribution parameters needed to describe the distribution of hop frequencies has been reduced to $\phi^i=\{f_l^i, f_h^i\}$. Equation (45) can be interpreted as the probability of occupancy of a portion of the spectrum centered around $f=f_n$ with bandwidth B_d by a continuous uniform random process. This interpretation is reasonable, since when the number of hopping channels is

large, the probability mass function of the hop frequencies is closely approximated using a continuous uniform random probability density function. This approximation will be used in the derivation of the frequency-based emission classification algorithm.

Let I be a random variable indicating which signal should be matched with a detected emission. If the emission in the n-th frequency bin is from the i-th FH signal, then $I=i$. If the probability of false alarm is assumed to be small, a bin is declared to be occupied only if an emission from a FH signal is present. The *signal match probability* (the probability that a detected emission is from the i-th FH signal given the data and knowledge of the distribution parameters) based on the frequency of a single emission is then given by

$$P[I=i|x(n)=1,\phi^1,\phi^2,\ldots,\phi^{N_s}]=\begin{cases}1 & \text{if } g(f_n|\phi^i)\neq 0\\ 0 & \text{OTHERWISE}\end{cases} \qquad (46)$$

Since the hopping spans of the FH signals do not overlap, the signal match probability is degenerate, and the emission frequency is sufficient for emission classification. The classification algorithm is equivalent to matching a detected emission to the FH signal that has a non-zero hop frequency distribution in the portion of the spectrum where the emission is located.

When the hopping spans of the signals overlap, the emission frequency no longer uniquely determines the FH signal of origin, but it does indicate which FH signal is more likely to have produced an emission.

Consider the classification problem when FH signals have overlapping but unequal hopping spans. For simplicity, suppose the receiver must classify a detected emission as being from one of two FH signals (N_s=2) using only the frequency of the emission (N_f=1, a single feature classification algorithm). The number of channels for both FH signals is assumed to be large, so a uniform distribution across the hopping span sufficiently describes the distribution of the hop frequencies. The distribution parameters for the classification algorithm are thus $\phi^i=\{f_l^i, f_h^i\}$, and the hop frequency distribution for each FH signal is given by

$$g(f_n|\phi^i)=\frac{1}{f_h^i-f_l^i}\zeta(f_l^i\le f\le f_h^i) \qquad (47)$$

As an example, let the distribution parameters for the two FH signals be $\phi^1=\{40,60\}$ and $\phi^2=\{55,65\}$ on an arbitrary frequency axis. Hop frequencies from the first FH signal assume values ranging from 40 to 60, while hop frequencies from the second FH signal assume values from 55 to 65.

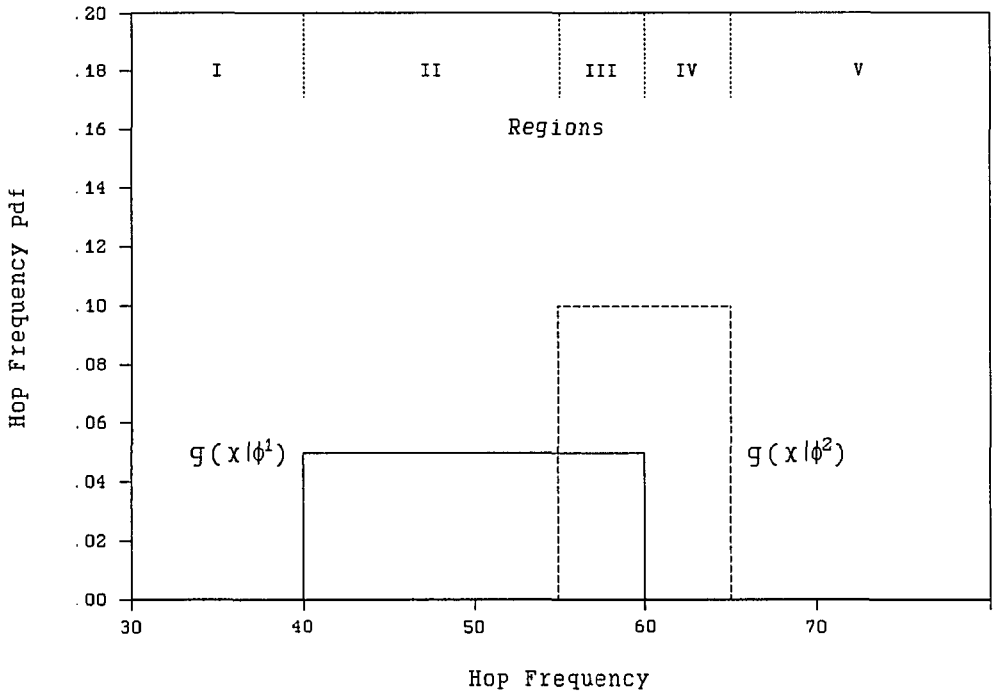

Figure 10. Hop frequency probability density functions for the two-signal example

There are five regions of interest, as shown in Figure 10. Regions I and V lie outside the hopping span of either FH signal. No emissions should be detected in either of these regions. An emission detected in region II is matched with the first FH signal with probability of one. An emission detected in region IV is likewise matched with the second FH signal, also with probability one. Because the hopping spans of the two FH signals overlap in region III, an emission detected in this region is potentially from either FH signal. However, the signal match probabilities for the two FH signals are not equal in this region, indicating that one

choice is preferred.

The probability of occupancy for any bin is $g(f_n|\phi^1)$ for the first signal and $g(f_n|\phi^2)$ for the second. By applying the law of total probability and using equation (45), the total probability of occupancy for a bin is

$$P[x(n)=1]=\sum_{i=1}^{N_s} g(f_n|\phi^i, I=i)\,P[I=i] \tag{48}$$

where $P[I=i]=1/N_s$ is the *a priori* probability that a detected emission is from the i-th FH signal. In region III, this function is evaluated as

$$P[x(n)=1]=\frac{1}{N_s}\left(\frac{B_d}{B_h^1}+\frac{B_d}{B_h^2}\right) \tag{49}$$

To calculate the probability that an emission from the i-th FH signal is present in the n-th bin, first note that if the hop frequencies from different FH signals are independent, the probability of occupancy conditioned on the signal being from the i-th FH signal is given by

$$P[x(n)=1\,|\,I=i,\phi^1,\phi^2,\ldots,\phi^{N_s}]=P[x(n)=1\,|\,I=i,\phi^i] \tag{50}$$

This implies that the sequence of hop frequencies from one FH signal is not influenced by the presence of other FH signals. Using this fact and Bayes rule, the signal match probability is $P[I=i|x(n)=1,\phi^i,\phi^2,\ldots,\phi^{N_s}]$, where

$$P[I=i|x(n)=1,\phi^1,\ldots,\phi^{N_s}]=\frac{P[x(n)=1|I=i,\phi^i]\,P[I=i|\phi^1,\ldots,\phi^{N_s}]}{P[x(n)=1]} \quad (51)$$

Equation (51) can be interpreted as the probability that an emission in the n-th bin is matched with the i-th signal given knowledge of the hopping spans of each FH signal. The expression $P[I=i|\phi^1,\ldots,\phi^{N_s}]$ represents the *a priori* probability that an emission located in the n-th bin is from the i-th signal, and is assumed to equal $1/N_s$. Using this assumption and the law of total probability, equation (51) can be rewritten as

$$P[I=i|x(n)=1,\phi^1,\phi^2,\ldots,\phi^{N_s}]=\frac{\frac{1}{N_s}P[x(n)=1|I=i,\phi^i]}{\sum_{m=1}^{N_s}P[x(n)=1|I=m,\phi^m]\,P[I=m,\phi^m]} \quad (52)$$

Equation (52) can be used to determine which FH signal an emission is most likely matched with. First, note that the probability of the n-th bin being occupied by the i-th FH signal, $P[x(n)=1|I=i,\phi^i]$, is equal to $g(f_n|\phi^1)$. From equation (45),

$$P[x(n)=1|I=i,\phi^i]=\begin{cases}\dfrac{B_d}{B_h^i} & f_l^i\le f_n\le f_h^i\\ 0 & \text{OTHERWISE}\end{cases} \quad (53)$$

In region III of the above example, the signal match probability is

$$P[I=i|x(n)=1,\phi^1,\phi^2] = \frac{\left(\frac{B_d}{B_h^i}\right)\left(\frac{1}{2}\right)}{\frac{1}{2}\left(\frac{B_d}{B_h^1}+\frac{B_d}{B_h^2}\right)} = \frac{B_h^1 B_h^2}{B_h^i (B_h^1+B_h^2)} \qquad (54)$$

The signal match probability is thus inversely proportional to the hop bandwidth, B_h^i, of the FH signal. Since the maximum likelihood criterion means emissions are classified as being from the FH signal with the largest signal match probability, equation (54) shows that in regions where hopping spans overlap, an emission is classified as being part of the FH signal with the smallest hop bandwidth. The signal match probability is only a function of the hop bandwidth (and span) of the FH signals and not the channel spacing.

The signal match probability given by equation (51) is valid in all regions of the spectrum, not just where the hopping spans of FH signals overlap. For example, in region II, $P[I=2|x(n)=1,\phi^1,\phi^2]=0$ and $P[I=1|x(n)=1,\phi^1,\phi^2]=1$. The signal match probability is equal to 0 when $i=2$, and 1 when $i=1$, so any emission detected in region II is classified as being from the first FH signal.

Figure 11 shows the signal match probabilities for each of the five regions obtained using equation (54), $B_h^1=(60-40)$

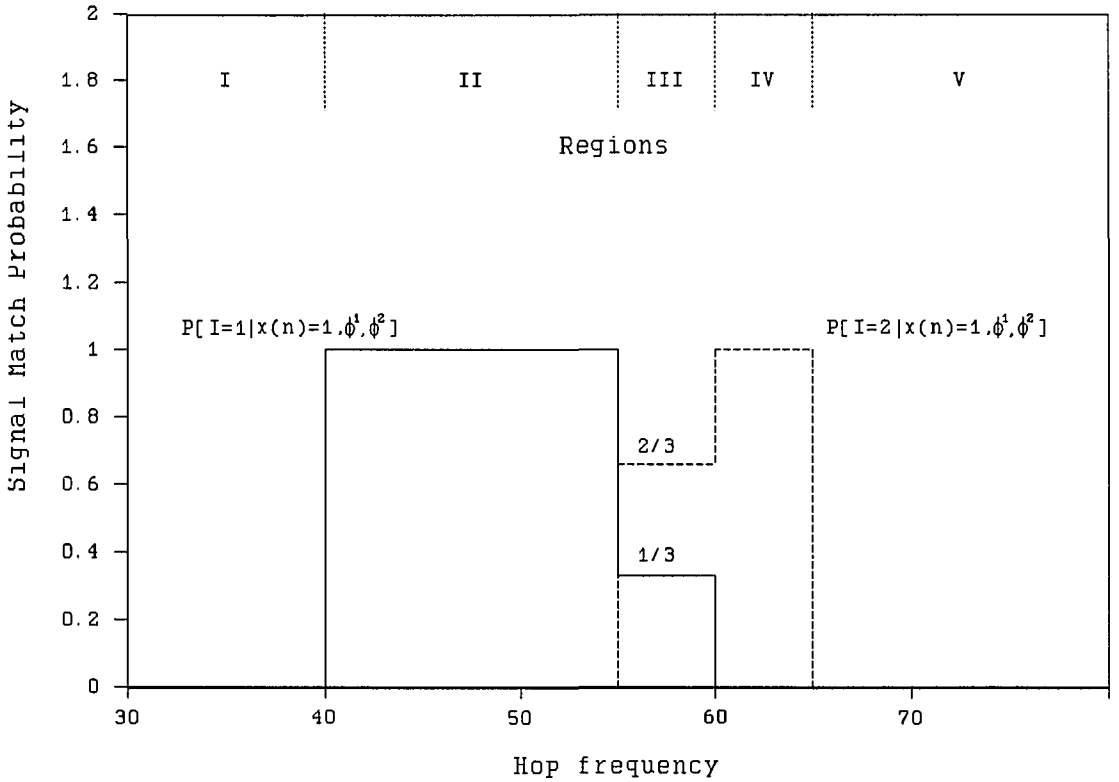

Figure 11. Signal match probability as a function of the emission frequency for the two-signal example

and B_h^2=(65-55). The preceding analysis provides a theoretical basis for quantifying the observation that an emission in region III is more likely to be from the second FH signal. Figure 11 shows that in region III, an emission is twice as likely to be from the second FH signal. In addition, the theoretical analysis agrees with the heuristic arguments in all other regions.

A short summary of the results of this section is useful. The maximum likelihood criterion dictates that a detected

emission should be matched with the FH signal with the largest signal match probability to minimize the probability of classification error. When emission frequency is used as data, this is equivalent to selecting the signal with the smallest hop bandwidth. In region III of the above example, signal 2 is selected as a match with detected emissions with a probability of 0.67 that the choice is correct. The high probability of error suggests that the emission frequency should not be used as the sole source of information, but as an additional source of information which has the potential to improve overall classification accuracy.

2. Emission classification using order statistics

In the previous section, known hopping spans were used to calculate the signal match probability which was found to be dependent only on the hopping spans of the FH signals. Because the hopping span of a FH signal is generally not known in advance, the intercept receiver must be capable of estimating the hopping span of each FH signal in order to classify emissions using frequency. In this section, the use of order statistics for estimating the hopping span of FH signals is examined.

When the hopping spans are not known, the intercept receiver estimates the signal match probability by calculating

$P[I=i|\hat{\phi}^1,\hat{\phi}^2,\ldots,\hat{\phi}^{N_s},x(n)=1]$, the probability that an emission in the n-th bin is part of the i-th FH signal using the distribution parameter estimates. The symbol "^" over a distribution parameter is used to denote an estimated quantity. Using Bayes rule and noting that $P[x(n)=1,\hat{\phi}^1,\hat{\phi}^2,\ldots,\hat{\phi}^{N_s}|I=i]=P[x(n)=1,\hat{\phi}^i|I=i]$ because data from different FH signals are independent, the estimate of the signal match probability is

$$P[I=i|x(n)=1,\hat{\phi}^1,\hat{\phi}^2,\ldots,\hat{\phi}^{N_s}]=\frac{P[x(n)=1,\hat{\phi}^i|I=i]\,P[I=i]}{P[x(n)=1,\hat{\phi}^1,\hat{\phi}^2,\ldots,\hat{\phi}^{N_s}]} \qquad (55)$$

As was the case with known hopping spans, $P[I=i]=1/N_s$ is interpreted as the *a priori* probability that a detected emission is part of the i-th FH signal. Since the hopping spans are not known, every FH signal must be considered a potential source of an emission.

The first term in the numerator of equation (55) can be interpreted as the probability of having an emission from the i-th FH signal present in the n-th bin and of having the current distribution parameter estimate. Let $\hat{\phi}_c^i$ be the distribution parameter estimate conditioned on the assumption that the emission is from the i-th FH signal. The first numerator term can be rewritten as

$$P[x(n)=1, \hat{\Phi}^i | I=i] = P[x(n)=1 | \hat{\Phi}_c^i] \, P[\hat{\Phi}^i | \hat{\Phi}_c^i] \tag{56}$$

The denominator of equation (55) can be viewed as a normalization factor by applying the law of total probability and noting that

$$P[x(n)=1, \hat{\Phi}^1, \hat{\Phi}^2, \ldots, \hat{\Phi}^{N_s}] = \sum_{m=1}^{N_s} P[x(n)=1, \hat{\Phi}^m | I=m] \, P[I=m] \tag{57}$$

which is the same for all FH signals.

A more useful expression for the estimate of the signal match probability is formed by substituting equations (56) and (57) into equation (55) and canceling common terms. The result of these operations is

$$P[I=i | x(n)=1, \hat{\Phi}^1, \hat{\Phi}^2, \ldots, \hat{\Phi}^{N_s}] = \frac{P[x(n)=1 | \hat{\Phi}_c^i] \, P[\hat{\Phi}^i | \hat{\Phi}_c^i]}{\sum_{m=1}^{N_s} P[x(n)=1 | \hat{\Phi}_c^m] \, P[\hat{\Phi}^m | \hat{\Phi}_c^m]} \tag{58}$$

To evaluate equation (58), the distribution of the distribution parameter estimates needs to be calculated. Let the number of emissions from the i-th FH signal detected by the receiver at the current epoch be denoted by N_e^i. The set of emission frequencies that have been observed from the i-th FH signal form a random sample of size N_e^i of independent random variables taken from a population with probability distribution function $g(f_n | \Phi^i)$.

The hopping spans are estimated using the smallest and largest hop frequencies observed from the FH signal. The smallest and largest hop frequency order statistics are simply the smallest and largest hop frequencies observed from a FH signal, or

$$\begin{aligned} a^i &= \min\{f_0^i + c_k^i B_c\} \\ b^i &= \max\{f_0^i + c_k^i B_c\} \end{aligned} \tag{59}$$

where f_0^i and c_k^i are the same quantities defined in equation (2) with the added superscript "i" used to indicate different FH signals. The order statistics a^i and b^i are consistent but biased estimators of f_1^i and f_h^i respectively.

The cumulative distribution functions of the order statistics are easily calculated from the cumulative distribution function for the hop frequencies. For the smallest hop frequency order statistic, the probability that any one hop frequency is greater than $f=b^i$ is $1-G(f|\phi^i)$. The probability that all N_e^i hop frequencies are greater than $f=b^i$ is this probability raised to the N_e^i-th power since the hop frequencies are assumed to be independently distributed. If the cumulative density function of the smallest hop frequency order statistic is represented by $G_{A^i}(f)$, this argument

results in the following expression:

$$1-G_{A1}(f)=(1-G(f|\phi^i))^{N_s^i} \tag{60}$$

Using a similar argument, the cumulative distribution function for the largest hop frequency order statistic is shown to be

$$G_{B1}(f)=(G(f|\phi^i))^{N_s^i} \tag{61}$$

For the specific example of hop frequencies with a uniform random distribution, the cumulative distribution function of the hop frequencies within the hopping span is given by

$$G(f|\phi^i)=\frac{f-f_l^i}{f_h^i-f_l^i} \qquad f_l^i \le f \le f_h^i \tag{62}$$

Substituting this function into equations (60) and (61), the distributions of the hop frequency order statistics are found to be

$$G_{A1}(f)=1-\left(\frac{f_h^i-f}{f_h^i-f_l^i}\right)^{N_s^i} \tag{63}$$

$$G_{B1}(f)=\left(\frac{f-f_l^i}{f_h^i-f_l^i}\right)^{N_s^i} \tag{64}$$

The hop frequency order statistics are computationally

efficient, because they can be recursively calculated and require minimal processing or storage. The hop frequency order statistics also converge rapidly due to the exponential dependence on the number of observed emissions.

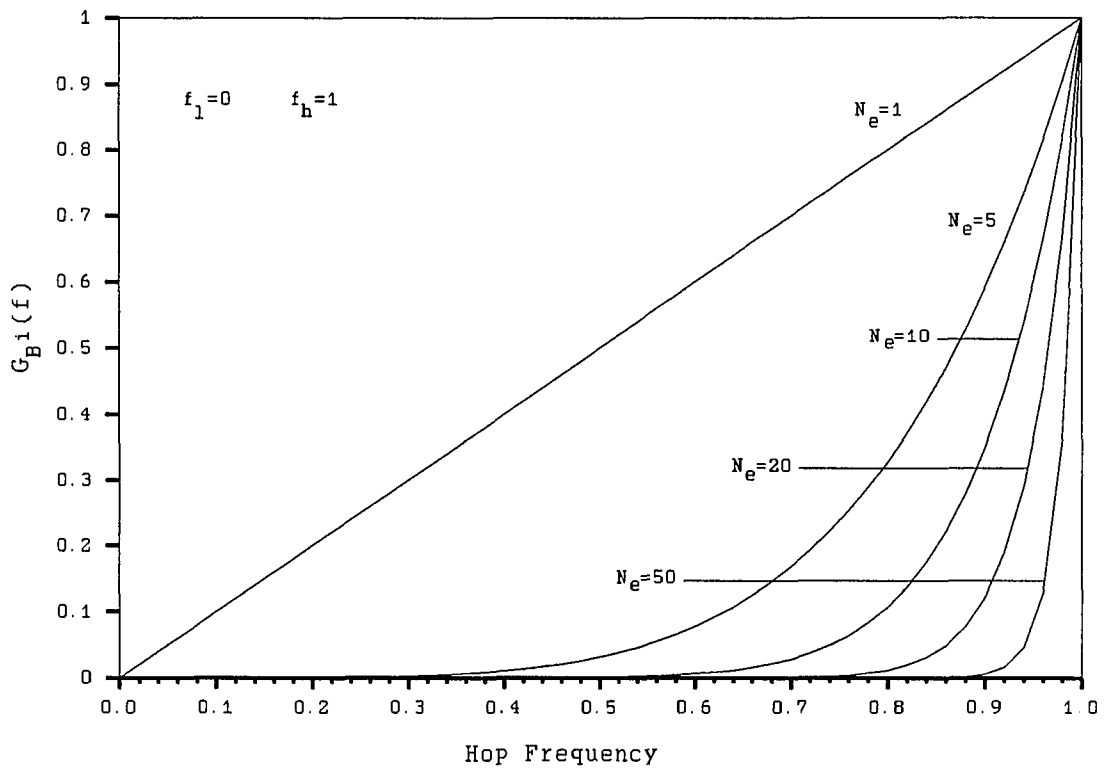

Figure 12. Cumulative distribution function for the largest hop frequency order statistic for 1,5,10,20, and 50 detected emissions

Figure 12 shows the cumulative distribution function for the largest hop frequency order statistic for different numbers of observed emissions. The hopping span has been normalized to $\phi^1=(0,1)$. After only 10 emissions, the median hop frequency order statistic encloses over 90 percent of the

hopping span. This demonstrates the efficiency of order statistics for interval estimation when the hop frequencies are uniformly distributed.

Let the conditional distribution parameter estimate, $\hat{\phi}_c^i$, be the estimate of the distribution parameter conditioned on the assumption that the emission detected at the frequency f_n is part of the i-th FH signal. When order statistics are used as the distribution parameter estimates, the conditional distribution parameter estimate is

$$\begin{aligned}\hat{\phi}_c^i &= \{ \min(a^i, f_n), \max(b^i, f_n) \} \\ &= \{a_c^i, b_c^i\}\end{aligned} \tag{65}$$

Having defined the *a priori* hop frequency distribution, the distribution parameters used by the receiver, the distribution of the distribution parameter estimates, and the conditional distribution parameter estimates, equation (58) can now be evaluated.

The conditional probability of occupancy of a frequency bin by an emission from the i-th FH signal is given by

$$P[x(n)=1 | \hat{\phi}_c^i] = \frac{B_d}{b_c^i - a_c^i} \tag{66}$$

The second term in the numerator of equation (58) is the probability of having the current distribution parameter estimates given the conditional distribution parameter

estimates. When order statistics are used as the distribution parameters, this quantity is equal to

$$P[\hat{\phi}^i|\hat{\phi}_c^i] = P[A^i=a^i, B^i=b^i|\hat{\phi}_c^i] \quad (67)$$

Using the joint probability of the largest and smallest order statistics, equation (67) is evaluated as

$$P[\hat{\phi}^i|\hat{\phi}_c^i] = \frac{N_e^i!}{(N_e^i-2)!} g(a^i|\hat{\phi}_c^i)\, g(b^i|\hat{\phi}_c^i)\left(G(b^i|\hat{\phi}_c^i) - G(a^i|\hat{\phi}_c^i)\right)^{N_e^i-2} \quad (68)$$

This rather formidable expression can be evaluated using equations (62) and (45). The resulting equations simplifies to

$$P[\hat{\phi}^i|\hat{\phi}_c^i] = \frac{N_e^i!}{(N_e^i-2)!}\left(\frac{B_d}{b_c^i-a_c^i}\right)^2\left(\frac{b^i-a^i}{b_c^i-a_c^i}\right)^{N_e^i-2} \quad (69)$$

Equation (69) is a function of the bandwidth computed using both the current distribution parameter estimates and the conditional distribution parameter estimates.

When the emission frequency lies within the estimated hopping span of the FH signal, $b^i-a^i=b_c^i-a_c^i$ and the last factor in equation (69) is unity. When the emission frequency lies outside of the estimated hopping span of a FH signal, $b^i-a^i < b_c^i-a_c^i$ and the probability of having the current estimate of the distribution parameters is less. As greater numbers of emissions from a FH signal are observed, equation

(69) rapidly converges toward zero for any emission frequency not contained within the estimate of the hopping span. The farther outside of the estimated hopping span the emission lies, the less likely it is to be from the signal. Also note that an inverse relationship to the hop bandwidth is still present, so FH signals with smaller hop bandwidths are still preferred over FH signals with larger hop bandwidths.

Using equations (69) and (45), the numerator of equation (58) is expressed as

$$P[x(n)=1|\hat{\phi}_c^i]\,P[\hat{\phi}^i|\hat{\phi}_c^i]=\frac{N_e^i!}{(N_e^i-2)!}\left(\frac{B_d}{b_c^i-a_c^i}\right)^3\left(\frac{b^i-a^i}{b_c^i-a_c^i}\right)^{N_e^i-2} \qquad (70)$$

The denominator can also be evaluated using equation (70), and an expression for the estimate of the signal match probability follows. The maximum likelihood criterion can then be applied to classify emissions.

To test the effectiveness of classification using emission frequency as a signal feature, a two signal, two parameter classifier was implemented and tested using computer simulation. The first signal feature was assumed to have a Gaussian distribution with known mean and variance. The Gaussian processes associated with the two signals were separated by 2 standard deviations. Using only these data and the maximum likelihood criterion, the probability of classification error is 0.159, which can be easily verified

from a table of areas under the normal curve.

The second signal feature used by the classifier was the hopping span of each FH signal. For this experiment, the two FH signals had equal hop bandwidths, $B_h^1=B_h^2=B_h$, separated by the hopping span offset, $d \cdot B_h$. The hopping span offset can be any positive value. The hop frequencies from both signals were uniformly distributed. The classification algorithm had no *a priori* knowledge of the distribution parameters. The experiment consisted of generating order statistics for each FH signal using the inverse CDF method, generating data using the signal features and their distributions, classifying each simulated emission and then updating the distribution parameter estimates based on the decision. The probability of classification error was found by averaging the results of many trials with the same hopping span offset.

When $d=0$, the hopping spans are completely superimposed and the emission frequency does not add any useful information. When $d \geq 1$ the hopping spans do not overlap, and the emission frequency is sufficient for error-free classification if the hopping spans are precisely known.

When both hopping spans are precisely known, the probability of classification error is linearly dependent on the offset between the hopping spans. When the hopping spans are superimposed, the probability of error is equivalent to

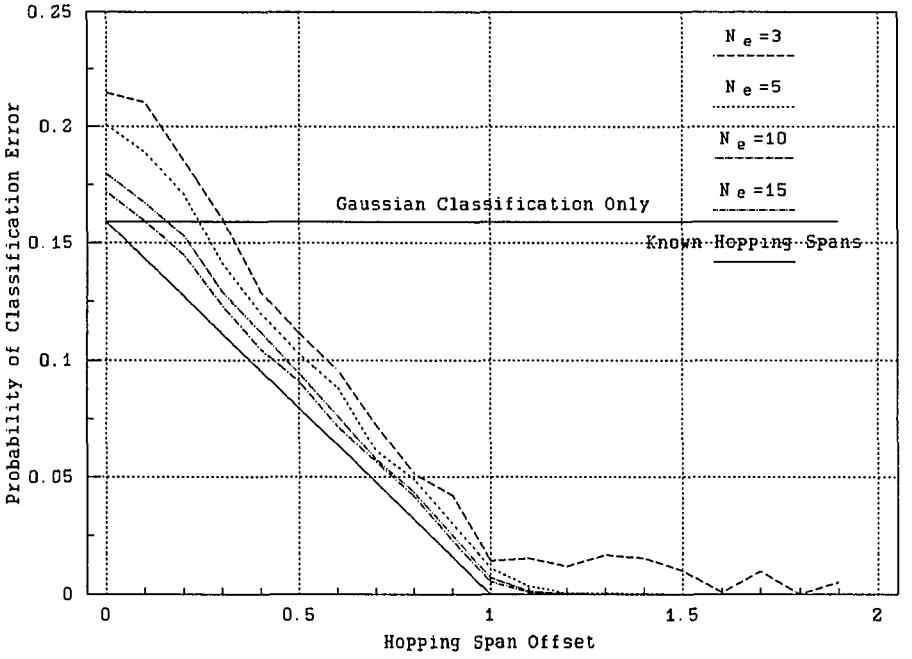

Figure 13. Experimental probability of sorting error using two signal parameters

the probability of error using just the normally distributed data, and decreases to zero linearly as the hopping span offset increases to one or more.

This result can be predicted by theory. When the hopping spans are known and hop bandwidths are equal, classification errors occur only in the region of the spectrum where hopping spans overlap. In this region, the signal match probabilities calculated using frequency are equal because the hop bandwidths of the FH signals are equal. The probability of error in this region is thus determined by the normally distributed signal feature. The overall probability of error is equal to the probability of error based on the normally

distributed data multiplied by the probability that an emission is in the region of the spectrum where hopping spans overlap. This leads to the following expression for the probability of classification error

$$P_{se}=\begin{cases} 0.159\,(1-d) & 0\le d\le 1 \\ 0.0 & d>1 \end{cases} \qquad (71)$$

When the hopping span estimates were initialized using N_e samples from the respective distributions, the results for N_e=15,10,5, and 3 are shown as the ascending lines in Figure 13. The probability of classification error still displayed a linear dependence on the hopping span offset, but the overall probability of error was increased. The increase in the level of error was caused by the uncertainty in the exact hopping spans of the two signals. The increase in the error was less when more correct data were used to initialize the hopping span estimates. This experiment shows that the hopping spans can be used as a signal feature, even when the spans are not known in advance. This experiment also demonstrates the importance of correct initialization of the distribution parameter estimates.

This experiment represents an extreme test of the classification algorithm since even when the distribution parameters are known, there can be up to a 0.159 probability of error. If the mean and variance of the Gaussian

distributions were not known in advance, it is very unlikely that the emissions could be classified with any degree of accuracy. The level of error can be reduced by either increasing the number of signal features, or by reducing the variance of the normally distributed data.

VI. EPOCH EMISSION CLASSIFICATION

In this chapter, a multiple emission classification algorithm is developed, and its relationship to the single emission classifier is discussed. An optimal two emission classification algorithm is developed using heuristic arguments and statistical theory, and its performance compared to the single emission classification algorithm. This algorithm is shown to significantly reduce the level of classification error present in the single emission classification algorithm. The two emission classification algorithm is then generalized to show the procedure for optimal classification of N_s emissions. Finally, the computational requirements of the classification algorithm are discussed, along with methods of reducing the requirements without degrading emission classification accuracy.

A. Two-Emission Classification Algorithm

While the single emission classification algorithm can be shown to minimize the probability of classification error, it uses no knowledge of other emissions present during an epoch. When multiple FH signals are present, classification errors are certain to occur when two or more emissions are matched

with the same FH signal during an epoch. By checking for multiple emissions assigned to a single FH signal, classification errors can be detected, and corrective action taken in many cases. Unfortunately, the single emission classification algorithm does not give any indication on how classification errors can be corrected. The multiple emission classification algorithm is designed to provide correct classifications in many instances when the single emission classification algorithm fails.

B. Single Feature Emission Classification

Consider an intercept receiver that classifies emissions using emission frequency, with the same hopping spans as shown in Figure 11. The decision rule from the previous chapter, obtained using the single emission classification algorithm, is that emissions in region II are matched with the first FH signal, and emissions in regions III and IV are matched with the second FH signal. The probability of emission classification error obtained using this method is 0.25 for emissions from the first FH signal (the probability that the hop frequency of the first FH signal lies within region III) and 0.00 for emissions from the second FH signal (because the maximum likelihood criterion classifies all emissions as being from the second FH signal in regions III and IV).

Common sense dictates that a lower level of emission classification error can be obtained by using information from all the emissions detected in an epoch together, rather than

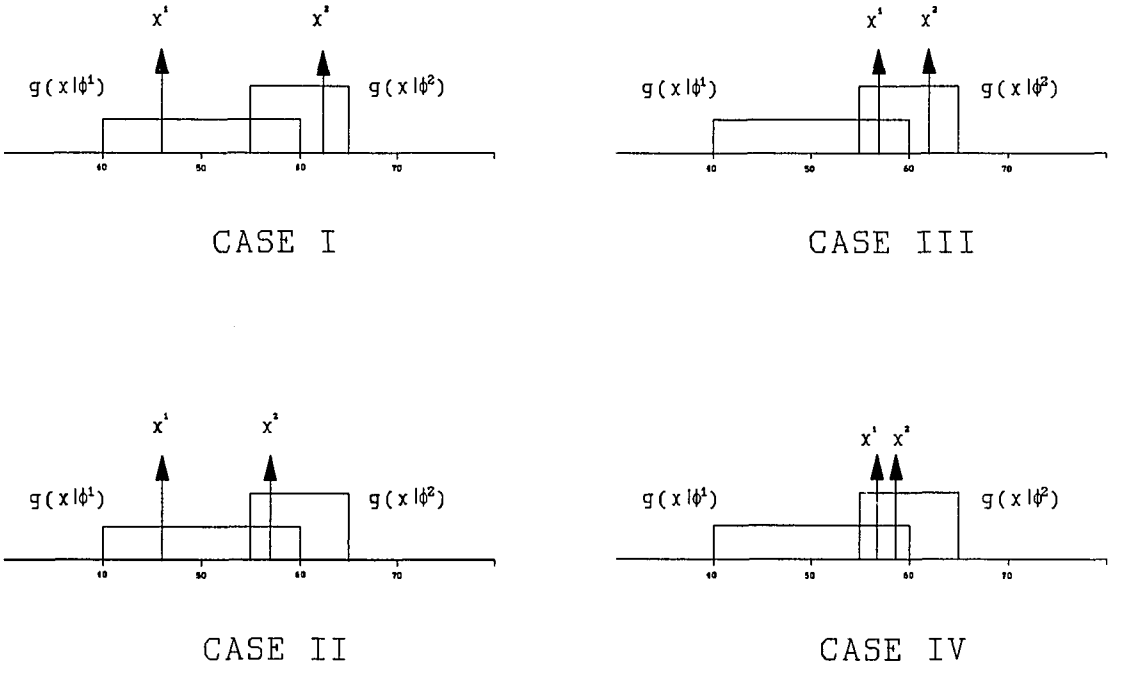

Figure 14. Four possible combinations of regions where emissions from the two FH signals can be located

by classifying based on knowledge of just a single emission. When emissions from both FH signals are detected, there are four possible combinations of regions where the two emissions can be located, as shown in Figure 14. Data from different signals are denoted using x^1 and x^2.

When emissions are present in regions II and IV (Case I), or II and III (Case II), no classification errors occur with

the single emission classification algorithm. When emissions are present in regions III and IV (Case III), or III and III (Case IV), both emissions are classified as being from the second FH signal. Error-free classification is still possible in case III since the emission in region IV can only be from the second FH signal. A known, but correctable, classification error occurs since two emissions are matched with the second FH signal by the classification algorithm. Only in case IV does an uncorrectable classification error occur. In this instance, using all the information from an epoch does not add any useful information. The single emission classification algorithm pairs both emissions with the second FH signal, and a known but uncorrectable classification error occurs.

The probability of classification error can clearly be reduced by using all data collected during an epoch. From the above discussion, uncorrectable classification errors occur only in case IV. Emissions from the first FH signal are present in region III with probability 0.25, and emissions from the second FH signal are present in this region with probability 0.50. The probability that both emissions are in region III is the product of these two numbers, or 0.125. The probability of an emission classification error using the heuristic algorithm developed above is thus 0.125, a reduction by a factor of two.

C. Epoch Emission Classification Algorithm

To provide a more rigorous analysis of the two emission classification algorithm, let n_1 and n_2 be bins containing emissions from the first and second FH signals respectively. The epoch classification algorithm has only two possibilities to choose from compared with four possibilities for the single emission classification algorithm. Either $I(n_1)=1$ and $I(n_2)=2$, or the converse is true. In a more general situation involving N_s FH signals, there are $N_s!$ permutations of emission/signal classifications from which to choose at each epoch.

An optimum classification algorithm bases its decisions on all data collected in a single epoch, instead of data from just one emission. In the two-emission single-feature sorting algorithm, the optimum classifier should therefore calculate $P[I(n_1)=i|x(n_1)=1,x(n_2)=1]$, the probability that the emission in the n_1-th bin is from the i-th FH signal given the frequency of both detected emissions. In the particular example being discussed, the receiver classifies the emission in bin n_1 by determining the value of i that maximizes $P[I(n_1)=i|x(n_1)=1,x(n_2)=1]$. This expression is easily evaluated using Bayes theorem, and can be written as

$$P[I(n_1)=i \mid x(n_1)=1, x(n_2)=1] = \frac{P[x(n_1)=1, x(n_2)=1 \mid I(n_1)=i]\, P[I(n_1)=i]}{P[x(n_1)=1, x(n_2)=1]} \quad (72)$$

The denominator of equation (72) can be viewed as a normalization term because it is not a function of i. The second term in the numerator, $P[I(n_1)=i]$, is the *a priori* probability that the emission in bin n_1 is from the i-th FH signal, and is assumed to be equal to $1/N_s$. Maximizing equation (72) is therefore equivalent to finding the value of i that maximizes $P[x(n_1)=1, x(n_2)=1 \mid I(n_1)=i]$. Using the independence of the FH signals, this can be rewritten as

$$P[x(n_1)=1, x(n_2)=1 \mid I(n_1)=i] = P[x(n_1)=1 \mid I(n_1)=i]\, P[x(n_2)=1 \mid I(n_1)=i] \quad (73)$$

When the signal feature is a known hopping span, equation (73) is equivalent to $g(f_{n_1} \mid \phi^1)\, g(f_{n_2} \mid \phi^2)$ when $i=1$ and $g(f_{n_1} \mid \phi^2)\, g(f_{n_2} \mid \phi^1)$ when $i=2$. In the two emission example, the epoch emission classification algorithm is shown to simplify to selecting the combination of signal/emission pairings that maximizes the product of the signal match probabilities.

Table 1 shows the four combinations of regions where emissions are present in the two-signal frequency-based example, and the test statistics for both possible hypotheses.

The test statistics are calculated using equation (47). Under hypothesis 0, emissions are correctly classified. Under hypothesis 1, both emissions are incorrectly classified. When knowledge of both detected emissions is used for classification, the correct choice is indicated (hypothesis 0 has the greater probability of occurring) in the first three cases.

Table 1. Signal match probabilities using the epoch classification algorithm and emission frequency as a signal feature

Emission Location		Hypothesis 0	Hypothesis 1
FH Signal 1	2	$g(f_{n_1}\|\phi^1)\,g(f_{n_2}\|\phi^2)$	$g(f_{n_2}\|\phi^1)\,g(f_{n_1}\|\phi^2)$
II	III	0.005	0.000
II	IV	0.005	0.000
III	IV	0.005	0.000
III	III	0.005	0.005

When both emissions are contained in region III, the epoch classification algorithm indicates that both hypotheses are equally likely, and either can be selected with equal probability of error. Suppose that in this instance, both emissions are classified as being from the second FH signal, which was the rule obtained from the single emission classification algorithm. The probability of classification error for the first FH signal is now the probability that both

emissions are present in region III, or 0.125. The probability of classification error for emissions from the second FH signal is still zero. The overall probability of classification error is the sum of these two numbers, or 0.125. The single emission sorting algorithm was previously found to have a probability of classification error equal to 0.250. By using knowledge of both emissions, the epoch classification algorithm has reduced the probability of classification error by a factor of two.

An interesting example that serves to illustrate how the epoch emission classification algorithm can improve classification accuracy occurs when classification is attempted using a single datum with a Gaussian distribution with known mean and variance. Let X^1 be normally distributed with mean $\mu^1<\mu^2$ and standard deviation σ_x. Let X^2 also be normally distributed with a different mean, μ^2, but the same standard deviation, σ_x. To classify the emissions, the classification algorithm must choose between the following hypotheses

$$\begin{aligned} H_0&: I(n_1)=1, I(n_2)=2 \\ H_1&: I(n_1)=2, I(n_2)=1 \end{aligned} \tag{74}$$

Using equation (73), the hypothesis test is equivalent to a test for distribution given by the product of the individual

signal match probabilities, or

$$e^{-\frac{1}{2}\left[\left(\frac{x(n_1)-\mu^1}{\sigma_x}\right)^2+\left(\frac{x(n_2)-\mu^2}{\sigma_x}\right)^2\right]} \underset{H_1}{\overset{H_0}{\gtrless}} e^{-\frac{1}{2}\left[\left(\frac{x(n_1)-\mu^2}{\sigma_x}\right)^2+\left(\frac{x(n_2)-\mu^1}{\sigma_x}\right)^2\right]} \tag{75}$$

This hypothesis test can be solved by using sufficient statistics. By taking the natural log of both sides and canceling common terms, the hypothesis test given by equation (75) simplifies to

$$x(n_2) \underset{H_0}{\overset{H_1}{\gtrless}} x(n_1) \tag{76}$$

This interesting result shows that when the epoch classification algorithm is used, the emission with the smallest data calculated from it is classified as being from the FH signal with the smallest mean. This decision rule is considerably different from the decision rule obtained using the maximum likelihood criterion and data from a single emission. There are no fixed decision regions. Instead, the observations are ordered, with the largest observation being matched with the FH signal with the larger mean.

The probability of error of the epoch classification algorithm is the average probability that an observation from the second FH signal is less than the observation from the first. Expressed in terms of the probability distribution functions of the data, the probability of classification error

is equal to the average probability that the datum from the second FH signal is less that the datum from the first FH signal, or

$$\frac{1}{\sqrt{2\pi}\sigma_x}\int_{-\infty}^{\infty}\left(\frac{1}{\sqrt{2\pi}\sigma_x}\int_{-\infty}^{x^1}e^{-\frac{1}{2}\left(\frac{x^2-\mu^2}{\sigma_x}\right)^2}dx^2\right)e^{-\frac{1}{2}\left(\frac{x^1-\mu^1}{\sigma_x}\right)^2}dx^1 \qquad (77)$$

The integral within the parenthesis in equation (77) is recognized as the probability that x^2 is less than x^1. This probability is multiplied by the probability of obtain that precise value of x^1, and integrated over all possible values to find the average likelihood that $x^2<x^1$.

Equation (77) is not readily evaluated, so numerical techniques were employed to calculate the probability of classification error. Figure 14 shows the log of the probability of classification error based on the normalized distance, $d=(\mu^2-\mu^1)/\sigma_x$, between the two processes, and the probability of classification error for both the single emission classification algorithm and the epoch emission classification algorithm. The epoch emission classification algorithm has significantly lower levels of error when compared with the single emission classification algorithm. The difference in the probability of classification error is least when the normalized distance is zero, and increases as the normalized distance increases.

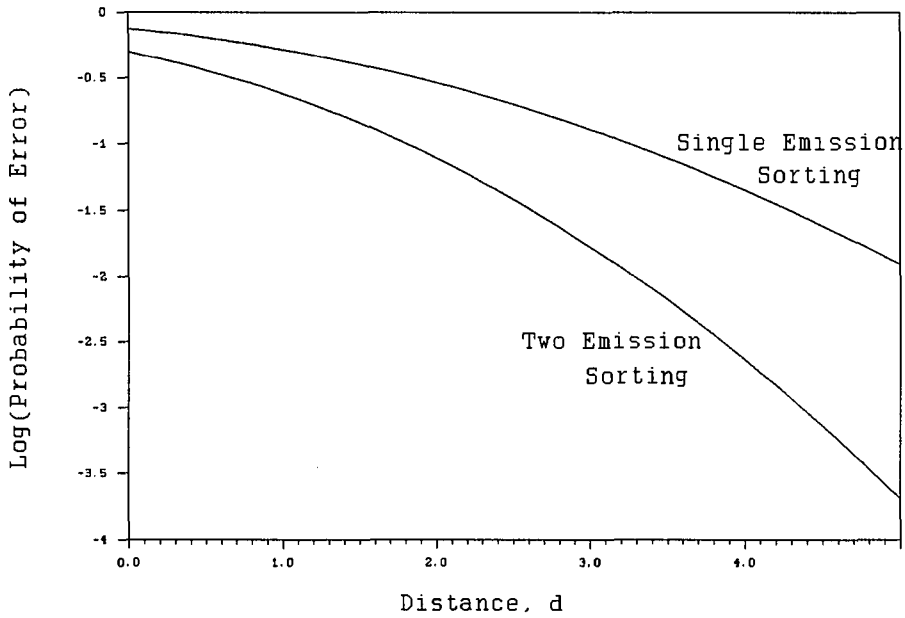

Figure 15. Log of the probability of error for the epoch emission classification algorithm, and the single emission classification algorithm

D. Two Emission, Multiple Feature Epoch Classification

The two-emission epoch classification algorithm outlined above can be generalized to include the case of multiple signal features calculated from each emission. At each epoch in which two emissions are detected, the receiver classifies emissions by solving the hypothesis test

$$P[\underline{x}(n_1)\,|\Phi^1]\,P[\underline{x}(n_2)\,|\Phi^2] \underset{H_1}{\overset{H_0}{\gtrless}} P[\underline{x}(n_2)\,|\Phi^1]\,P[\underline{x}(n_1)\,|\Phi^2] \qquad (78)$$

when the distribution parameters are known. When the distribution parameters are not known in advance, estimates of

the signal match probability given by equation (58) are used instead.

Returning to the two-signal, two-feature example used to produce the results of Figure 13, the same system was used as input to a two feature epoch classification algorithm. Figure 16 shows the experimentally determined probability of classification error obtained using the epoch classification algorithm. The distribution parameter estimates were initialized with 2, 5, 10, and 15 correctly-classified emissions before the classification algorithm was used.

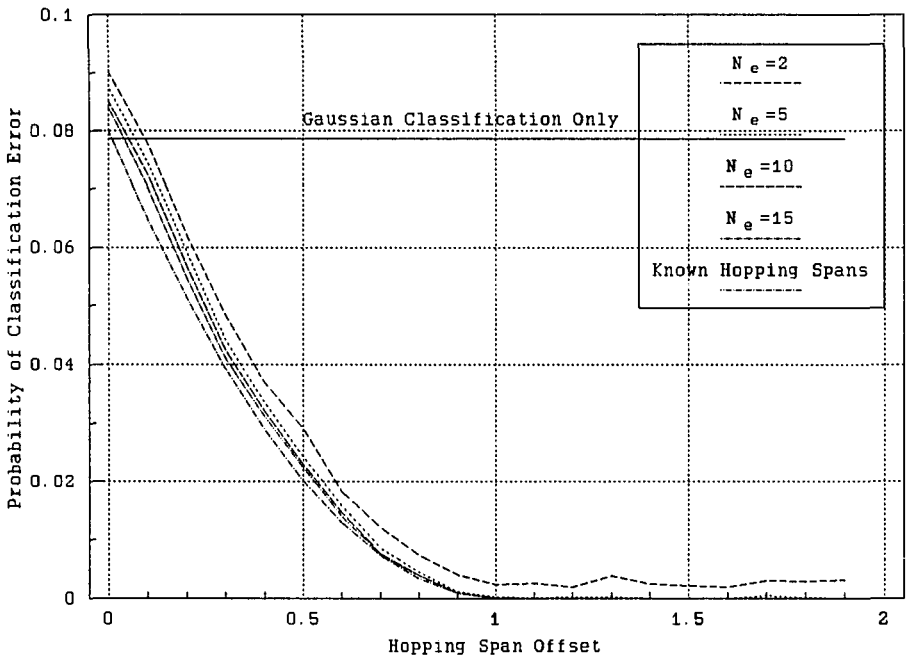

Figure 16. Probability of classification error for the epoch emission classification algorithm using normally distributed data and emission frequency as data

Comparison of Figure 16 with Figure 13 shows that the probability of classification error has been reduced by approximately a factor of two overall.

When classifying emissions using only the normally distributed data, the probability of classification error is exactly one half of that obtained using single emission classification. When the offset increases to the point where the hopping spans are adjacent, the probability of classification error is closely approximated by a quadratic. The decrease in classification error was linear with the single emission sorting algorithm, so not only is the probability of classification error less, but it also approaches zero faster with increasing hopping span offset.

Reduction in the level of classification error is due both to the greater accuracy of the epoch classification algorithm, and to the better signal feature estimates which are created as a consequence of more accurate emission classifications. The epoch classification algorithm is also less dependent on correct initialization of the distribution parameter estimates, since the probability of classification error is less sensitive to the number of correctly classified emissions used to initialize these estimates. The epoch classification algorithm is thus more robust and less subject to problems arising from incorrect classifications during the first few emissions observed from a FH signal.

E. Multi-Emission and Feature Epoch Classification

In this section, the epoch classification algorithm is generalized to classify an arbitrary number of emissions. The form of the optimal classification algorithm for N_s FH signals is examined. As will be shown, the test statistic for a multi-emission, multi-feature epoch classification algorithm can still be written in terms of the signal match probability for a single emission, but it does not have the simple form of the two emission classification algorithm.

To determine the form of the test statistic for a general epoch classification algorithm, it is instructive to look at the probability that an emission is from the i-th FH signal using information from all detected emissions in an epoch. This probability can be expressed as

$$P[I(n_1)=i|\underline{x}(n_1),\underline{x}(n_2),\ldots,\underline{x}(n_{N_s})] = \frac{P[\underline{x}(n_1),\underline{x}(n_2),\ldots,\underline{x}(n_{N_s})|I(n_1)=i]\,P[I(n_1)=i]}{P[x(n_1)=1,x(n_2)=1,\ldots,x(n_{N_s})=1]} \quad (79)$$

The denominator of the above expression is independent of i, and serves as a normalization term. The function $P[I(n_1)=1]$ represents the *a priori* probability that an emission is from the i-th FH signal, and is also assumed to be independent of i. Thus, equation (79) can be maximized by

finding the value of i that maximizes the first term in the numerator. Using the independence of the random processes from different FH signals, this term can be rewritten as

$$\begin{aligned} &P[\underline{x}(n_1),\underline{x}(n_2),\ldots,\underline{x}(n_{N_s})\,|\,I(n_1)=i] = \\ &\quad P[\underline{x}(n_1)\,|\,I(n_1)=i]\,P[\underline{x}(n_2),\underline{x}(n_3),\ldots,\underline{x}(n_{N_s})\,|\,I(n_1)=i] \end{aligned} \tag{80}$$

The first term can be evaluated easily using the relationship $P[\underline{x}(n_1)\,|\,I(n_1)=i]=P[\underline{x}(n_1)\,|\,\underline{\Phi}^i]$ and equation (37). The second term represents the probability of obtaining the remaining data given that none of the emissions are from the i-th FH signal. When there are only two signals, the second emission is classified by default. When there are more than two emissions, the second numerator term is not as easy to evaluate. Through repeated applications of the law of total probability, this term can be rewritten as

$$\begin{aligned} &P[\underline{x}(n2),\underline{x}(n_3),\ldots,\underline{x}(n_{N_s})\,|\,I(n_1)=i] = \\ &\quad \sum_{\substack{i2=1\\ i2\neq i}}^{N_s} \frac{P[\underline{x}(n_2)\,|\,I(n_2)=i2]}{N_s-1} \\ &\qquad \sum_{\substack{i3=1\\ i3\neq i2\\ i3\neq i}}^{N_s} \frac{P[\underline{x}(n_3)\,|\,I(n_3)=i3]}{N_s-2} \\ &\qquad\qquad \vdots \\ &\qquad\qquad P[\underline{x}(n_{N_s})\,|\,I(n_{N_s})=i_{N_s}] \end{aligned} \tag{81}$$

Equation (81) is a series of nested summations used to evaluate the probability that the remaining emissions are from

any but the i-th FH signal. Its function is to reduce classification errors by considering the probability of the remaining classifications. For example, if N_s=3 and i=1, equation (81) is equal to

$$\begin{aligned} &P[\underline{x}(n_2), \underline{x}(n_3) \,|\, I(n_1)=1] = \\ &\quad \frac{1}{2} P[\underline{x}(n_2) \,|\, I(n_2)=2]\, P[\underline{x}(n_3) \,|\, I(n3)=2] + \\ &\quad \frac{1}{2} P[\underline{x}(n_2) \,|\, I(n_2)=3]\, P[\underline{x}(n_3) \,|\, I(n_3)=2] \end{aligned} \tag{82}$$

If the emission in bin n_1 is from the first FH signal, there are two possibilities for the remaining emissions. Either $I(n_2)$=2 and $I(n_3)$=3, or $I(n_2)$=3 and $I(n_3)$=2. Since there are only two possibilities, the *a priori* probability of each is assumed to be one-half.

When N_s=2, equation (79) is equal to

$$\begin{aligned} &P[I(n_1)=i \,|\, \underline{x}(n_1), \underline{x}(n_2)] = \\ &\qquad \frac{P[\underline{x}(n_1), \underline{x}(n_2) \,|\, I(n_1)=i]\, P[I(n_1)=i]}{P[x(n_1)=1, x(n_2)=1]} \end{aligned} \tag{83}$$

which is identical to the two-emission epoch classification algorithm given by equation (72). Unfortunately, the number of computations needed for each emission increases rapidly with the number of FH signals. The computational requirements of the classification algorithm are a concern, since emission feature estimation and classification must take less time than

an epoch to complete.

F. Multiple-Emission, Multiple-Feature Simulation

A simulation of the RF environment was created to test the accuracy of the epoch emission classification algorithm in a realistic signal environment. A simulation was used because of the difficulty in obtaining an analytical solution in all but the most elementary situations. In addition, the simulation provided useful experience with factors not included in the analytical model such as the presence of fixed-frequency signals, collisions in frequency of two FH signals, and signal feature initialization and estimation.

Up to 25 FH signals were present in the simulation, although no more than 5 FH signals were allowed to have non-zero amplitude functions at a time. The number of FH signals active at any epoch, N_s, was always less than or equal to five. The number of FH signals active during an epoch was estimated by the receiver, since it was provided with no *a priori* information. The only constraints placed on the FH signals by the simulation were (1) dwell times were longer than a single epoch, (2) dwells were an integer number of epochs long, and (3) the hopping bandwidth was entirely contained within the frequency span analyzed by the intercept

receiver. A signal magnitude versus frequency display of an RF environment created by the simulation was previously shown in the bottom of Figure 2.

An N_f=4 feature classification algorithm was implemented for the simulation. The data used by the classification algorithm were emission frequency, epoch-of-arrival, signal magnitude, and azimuthal angle-of-arrival. The algorithm for exploiting the emission frequency was presented previously. The epoch-of-arrival was assumed to have a degenerate distribution. The remaining data were assumed to have Gaussian distributions with known variances but unknown means. To reduce the computational requirements of the simulation, a two-step method for emission classification was devised. The single emission classification algorithm was used until an error was detected. The epoch classification algorithm was then used to resolve those errors.

The effect of the epoch classification algorithm was to minimize the probability of a classification error or errors occurring in an epoch. This contrasts with the single emission classification algorithm, which minimizes the probability of classification error for an emission using just the data calculated from the emission. Figure 17 shows a histogram of the number of transmissions with the same percentage of correctly classified emissions. A transmission

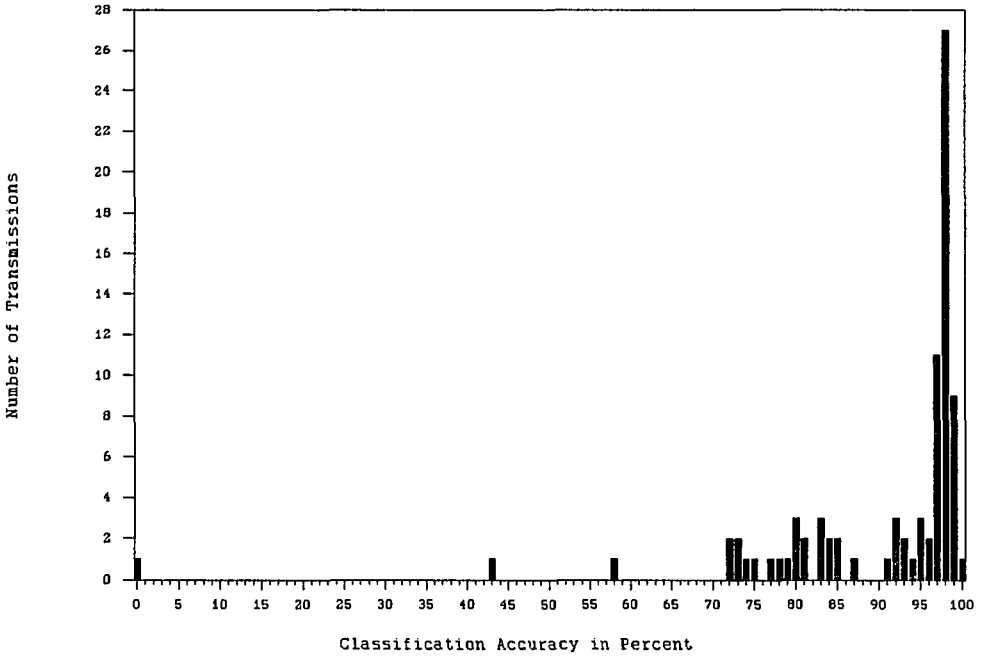

Figure 17. Histogram of classification accuracy obtained from the simulation

refers to a portion of a FH signal where the amplitude function is non-zero. The figure suggests that emission classification can be quite accurate using just a few signal feature estimates.

The results of the simulation also show that there are several factors which influence classification accuracy aside from the number of features used by the classification algorithm. Another determining factor is the quality of the distribution parameter estimates. When the distribution parameters are not known in advance but are estimated from past decisions, the quality of the estimates is determined by the quality of the signal feature estimates and the accuracy

of the classification algorithm--especially in the first few dwells detected from a FH signal. High quality data increase the percentage of correct classifications and the quality of the distribution parameter estimates. Other factors determining classification accuracy are the total number of signals present, both FH and fixed frequency, and the amount of "separation", in information space, between features of different signals.

When the emission classification accuracy is above approximately 90 percent, the classification algorithm is successful. The vast majority of the transmissions shown in Figure 17 are in this category. Classification errors occurred only during collisions in frequency between emissions from two or more FH signals, or between an emission from a FH signal and a strong, fixed-frequency signal. In the event that there were no collisions in frequency during a transmission, classification accuracies of 100 percent were achieved.

When the emission classification accuracy was between 70 and 90 percent, FH emissions were not being properly classified in portions of the spectrum occupied by low-power fixed-frequency signals. This occurred if the FH signal had a very low amplitude, or if its features were close to the features of a fixed-frequency signal. The classification accuracy could be improved by either (1) improving the

accuracy of the data (thereby increasing the separation in information space), or (2) by using additional signal features for classification.

The two transmissions with emission classification accuracies near 50 percent had nearly identical signal features. The classification algorithm consequently interchanged emissions from the two transmissions. To make this scenario less probable, either the data quality should be improved or the number of signal features used by the receiver should be increased.

Finally, a lone transmission is shown with an emission classification accuracy near zero. When this situation occurred, the cause was inevitably attributable to either a failure to initialize properly (which represents a short period of time of the total transmission) or a failure of the algorithm which was used to evaluate the classification accuracy.

The epoch emission classification algorithm can never be guaranteed not to fail, since a scenario can always be envisioned where the data used for classification are not sufficient. However, failures, when they occur, do not have catastrophic consequences. Instead, they tend to gradually degrade the accuracy of the classification algorithm. The vast majority of the transmissions had small to moderate levels of classification error. This simulation has shown the

algorithm to be extremely robust and accurate.

VII. CONCLUSIONS

Spread spectrum modulation was developed as a means of providing secure, interference-resistant communications. Several different methods of spread spectrum modulation are currently used for military, commercial, and experimental communications. Powerful new digital signal processors open the possibility that the security and anti-interference properties of frequency hopped spread spectrum modulation can be diminished. In this dissertation, a new method of defeating frequency-hopped spread spectrum modulation using fast spectral analyses and emission classification was proposed. Spectral analyses were used to detect emissions from FH signals, while the classification algorithms were used to identify emissions from the same FH signal.

Both analog and digital radiometric receivers were examined. A digital receiver is more practical than an analog intercept receiver because it does not require numerous analog bandpass filters. Also, samples of the received signal used to calculate the periodogram can be stored and used again to calculate data for the classification algorithm. The epoch length of the digital receiver is limited by the time required to sample and analyze the data. Large FFT's are needed to achieve fine spectral resolution, but require greater processing power, and longer observation times than smaller

FFT's. To avoid complications that arise because the intercept receiver is not synchronized with the FH signal, the observation time in an intercept receiver should be less than the smallest expected dwell time. To meet this criterion, a digital intercept receiver must either have a coarser frequency resolution than an optimal receiver, or use parallel processing to analyze delayed versions of the input.

The theoretical foundations of Baysian analysis and the application of this theory to the emission classification problem was described. A maximum likelihood emission classification algorithm using data with arbitrary distributions was outlined. Several examples were given to illustrate how the algorithm performed in simple situations. The effects of key factors affecting emission classification accuracy such as the number of features used by the receiver and data accuracy were discussed. An epoch-level emission classification algorithm was presented. The epoch-level emission classification algorithm was found to perform significantly better than the maximum likelihood algorithm, but is significantly more complex--especially if the number of data used for classification or the number of signals are large.

In a computer simulation designed to determine the classification accuracy in a realistic signal environment, classification accuracies of up to 100 percent were observed.

The classification accuracy was frequently over 90 percent--even when 30 percent of the detector bins were occupied. Baysian classification combined with radiometric detection was found to be an effective means of defeating FH modulation.

Because implementation of a digital intercept receiver requires the use of technology and techniques that are just becoming practical, numerous research opportunities exist. While the subjects cannot be considered separately, these opportunities are in the areas of signal analysis and emission classification.

In signal analysis, a rudimentary algorithm for detecting sinusoids in white noise was presented. Although mathematically tractable, this model is not likely to accurately depict the spectrum that would be encountered by an intercept receiver. The presence of wideband, low-power signals such as direct sequence transmissions or television broadcasts was not taken into account by this first analysis. In addition, the hopping bandwidth that must be analyzed is extremely large, and there is a possibility that the noise spectrum may not be flat. Separate processors operating on the output of each frequency bin may be necessary for improved signal detection. Research into the probability of detection for modulated signals, the effects of bin spreading, finite-resolution samples, and detection algorithms for sinusoids in colored noise or time-variant low-power signals all need to be

investigated.

In the area of signal classification, classification techniques and data estimation both need further research. This research could be extended by looking at different choices for the cost function and *a priori* probabilities to lower the probability of classification error. Also of interest is determining what signal features are most useful in classifying emissions, and how many features need to be used for accurate sorting under the conditions most likely to be encountered. Non-Baysian classification techniques could also be attempted.

Although many questions remain to be addressed, this research demonstrated the feasibility of defeating frequency-hopped spread spectrum modulation using Baysian classification, and has laid the groundwork for future research activity.

VIII. BIBLIOGRAPHY

[1] Raymond L. Pickholtz, Donald L. Schilling and Laurence B. Milstein. "Theory of Spread-Spectrum Communications--A Tutorial." IEEE Trans. on Communications, COM-30, No. 5 (May 1982): 855-884.

[2] Robert A. Scholtz. "The Origins of Spread-Spectrum Communications." IEEE Trans. on Communications, COM-30, No. 5 (May 1982): 822-854.

[3] C. E. Shannon. "A mathematical theory of communication." Bell Syst. Tech. J., Vol. 28 (October 1949): 379-423.

[4] Robert C. Dixon. Spread Spectrum Systems. New York, John Wiley and Sons, 1984.

[5] Klaus M. Dostert. "Frequency-Hopping Spread-Spectrum Modulation for Digital Communications Over Electrical Power Lines." IEEE Journal on Selected Areas in Communications, SAC-8, No. 4 (May 1990): 700-710.

[6] Harry Urkowitz. "Energy Detection of Unknown Deterministic Signals." Proceedings of the IEEE, Vol. 15, No. 4 (April 1967): 523-531.

[7] Robin A. Dillard and George M. Dillard. Detectability of Spread-Spectrum Signals. Norwood, Artech House, 1989.

[8] George R. Cooper. "Detection of Frequency-Hop Signals." MILCOM, 1986.

[9] Marvin K. Simon, Jim K. Omura, Robert A. Scholtz, and Barry K. Levitt. Spread Spectrum Communications. Rockville, Computer Science Press, 1985.

[10] William A. Gardner. "Signal Interception: A Unifying Theoretical Framework for Feature Detection." IEEE Trans. on Communications, COMM-36, No. 8 (August 1988): 897-906.

[11] Andreas Polydoros and Chrysostomos L. Nikias. "Detection of Unknown-Frequency Sinusoids in Noise: Spectral Versus Correlation Domain." IEEE Trans. on Acoustics, Speech, and Signal Processing, ASSP-35, No. 6 (June 1987): 897-900.

[12] Robin A. Dillard. "Detectability of Spread-Spectrum Signals." IEEE Trans. on Aerospace and Electronic Systems, AES-15, No. 4 (July 1979): 526-537.

[13] William E. Snelling and Evaggelos Geraniotis. "Sequential Detection of Unknown Frequency-Hopped Waveforms." IEEE Journal on Selected Areas in Communications, SAC-7, No. 5 (May 1989): 602-605.

[14] Norman C. Beaulieu, Wendy L. Hopkins, and Peter J. McLane. "Interception of Frequency-Hopped Spread-Spectrum Signals." IEEE Journal on Selected Areas in Communications, SAC-8, No. 5 (June 1990): 853-870.

[15] Andreas Polydoros and Kai T. Woo. "LPI Detection of Frequency-Hopping Signals Using Autocorrelation Techniques." IEEE Journal on Selected Areas in Communications, SAC-3, No. 5 (September 1985): 714-726.

[16] George R. Cooper, and Robert D. Martin. "Detection and Identification of Multiple Spread-Spectrum Signals." MILCOM, 1990.

[17] William E. Snelling and Evaggelos A. Geraniotis. "The Optimal Interception of Frequency-Hopped Waveforms via a Compressive Receiver." MILCOM, 1990.

[18] Jackie E. Hipp. "Modulation Classification based on Statistical Moments." MILCOM, 1986.

[19] F. F. Liedtke. "Computer Simulation of an Automatic Classification Procedure for Digitally Modulated Signals with Unknown Parameters." Signal Processing, SP-6, pp. 311-323, 1984.

[20] Andreas Polydoros and Kiseon Kim. "On the Detection and Classification of Quadrature Digital Modulations in Broad-Band Noise." IEEE Trans. on Communications, COMM-38, No. 8 (August 1990): 1199-1211.

[21] Shue-Zen Hsue and Samir S. Soliman. "Automatic Modulation Recognition of Digitally Modulated Signals." MILCOM, 1989.

[22] Ralph O. Schmidt. "Multiple Emitter Location and Signal Parameter Estimation." IEEE Trans. on Antennas and Propagation, AP-34, No. 3 (March 1986): 276-280.

[23] David L. Nicholson, Stephan D. Huffman, James H. Shattuck, and Daniel F. Lyons. "Emitter Sorting Using a Multi-Dimensional Vector of Signal Features." MILCOM, 1987.

[24] B. L. Connelly and B. W. Kroeger. "Design and Performance of an Analysis Receiver." MILCOM, 1990.

[25] John Kellor. "From TRW, The First SuperChip." Military and Aerospace Electronics, 2 (February 1990): 1.

[26] J. L. Melsa and D. L. Cohn. Decision and Estimation Theory. New York, NY: McGraw-Hill, 1978.

[27] Bernard W. Lindgren. Statistical Theory. New York, Macmillan Publishing Company, 1976.

[28] Thomas Shelburne Ferguson. Mathematical Statistics, a Decision Theoretic Approach. New York, Academic Press 1967.

[29] Alan V. Oppenheim and Ronald W. Schafer. Digital Signal Processing. Englewood Cliffs, Prentice-Hall, 1975.

[30] Murat Kunt. Digital Signal Processing. Norwood, Artech House, 1986.

[31] William H. Press, Brian P. Flannery, Saul A. Teukolsky, and Willian T. Vetterling. Numerical Recipes--The Art of Scientific Computing. Cambridge, Cambridge University Press, 1989.

IX. GLOSSARY OF SYMBOLS

$A(t)$	amplitude function
A^i	smallest hop frequency order statistic
B^i	largest hop frequency order statistic
B_c	channel spacing
B_h	hop bandwidth
B_d	signal detector bandwidth
$\{c_k\}$	pseudo-random spreading code
$d(x)$	decision
$d_b(x)$	Bayes rule
$E_s(n)$	signal power in the n-th bin
$f_0+c_kB_c$	hop frequency
f_l	lower limit of the hopping span
f_h	upper limit of the hopping span
$g(\cdot)$	probability distribution function of the data
$G(\cdot)$	cumulative distribution function of the data
$G_{A^i}(f)$	smallest hop frequency order statistic CDF
$G_{B^i}(f)$	largest hop frequency order statistic CDF
H_j	j-th hypothesis
i	FH signal index
I	random variable denoting which FH signal an emission is from
j	receiver decision of the FH signal which produced an FH signal
k	dwell index
$L(\cdot,\cdot)$	loss function
N_c	number of channels
N_s	number of FH signals present
N_e^i	number of emissions observed from the i-th FH signal
N_f	number of features used for classification
N_0	single sided noise power spectral density
$n(t)$	additive noise
Q^i	sufficient statistic
$R(\cdot,\cdot)$	risk , and FFT of the received signal
$R'(\cdot,\cdot)$	FFT of the frequency-shifted received signal
$r(\cdot,\cdot)$	Bayes risk
$R(f)$	Fourier transform of the received signal
$R'(\cdot)$	Fourier transform of the frequency-shifted signal
$r(t)$	received signal

$r'(t)$	frequency-shifted received signal
$s(t)$	FH signal
$s_k(t)$	gated fixed frequency signal
$V(t)$	analog radiometer output
$W(n,\epsilon)$	periodogram
$W(n)$	periodogram suppressing the epoch dependency
$Y(n)$	spectral amplitude of a noise shaping filter
ϕ^i	distribution parameter
$\hat{\phi}^i$	distribution parameter estimate
$\pi(\cdot)$	prior distribution
η	detection threshold
x	data
$\rho(\cdot)$	unit pulse function
τ_c	dwell time
ϵ	epoch index
$\theta(t)$	phase function
σ_m^i	standard deviation of a Gaussian random variable
μ_m^i	mean of a Gaussian random variable
$\zeta(\cdot)$	indicator function

X. APPENDIX A: DETECT.FOR

```
C*** DETECT.FOR ***********************************************
C
C  FUNCTION    - CALCULATE PROBABILITY OF DETECTION FOR SIGNALS
C                USING A DFT FOR SPECTRAL ANALYSIS.  INPUT IS
C                OF DIFFERENT AMPLITUDE SINUSOIDS AT THE
C                DISCRETE FREQUENCIES OF THE DFT.
C
C  PRECISION   - SINGLE
C
C  REQ'D ROUTINES
C              - REALFT - COMPUTES THE FOURIER TRANSFORM
C                OF A REAL SEQUENCE.  FROM NUMERICAL RECIPES
C                GASDEV - GAUSSIAN RANDOM NUMBER GENERATOR.
C                FROM NUMERICAL RECIPES
C
C  PROGRAMMER - J. ERIC DUNN
C                DEPT OF ELECTRICAL AND COMPUTER ENGINEERING
C                IOWA STATE UNIVERSITY    (GO CLONES!)
C                AMES, IOWA 50011
C                (515)294-3966
C
C  LAST REVISION  8/23/90
C *************************************************************
C
      REAL X(512),PFA(5),S(512)
      OPEN(UNIT=10,FILE='PWRSAMP.DAT')

C USE 4 DIFFERENT PROBABILITIES OF FALSE ALARM
      PFA(1)=0.01
      PFA(2)=0.001
      PFA(3)=0.0001
      PFA(4)=0.00001

      ARG=0.122718463

      DO 2 K=1,4
C ENERGY DETECTION THRESHOLD
        ETA = -0.25 * LOG(PFA(K))
C SNR IN DBS
        DO 3 AMP=0,2,0.25
C CALCULATE AMPLITUDE
          FACTOR= 10**AMP
C DO MONTE-CARLO SIMULATION
        DO 10 I=1,2500
C GENERATE THE SEQUENCE
          DO 20 J=1,512
20      X(J) = FACTOR*(0.001*SIN(ARG*J)+
```

```
     &          0.002*SIN(ARG*3*J)+
     &          0.003*SIN(5*ARG*J) +
     &          0.004*SIN(7*ARG*J) +
     &          0.005*SIN(9*ARG*J) +
     &          0.006*SIN(11*ARG*J) +
     &          0.008*SIN(13*ARG*J)) +
     &          0.50 * GASDEV(IDUM)
C COMPUTE THE FOURIR TRANSFORM
          CALL REALFT(X,256,1)
C CALCULATE THE PERIODOGRAM TEST VALUES
          T1=(X(21)**2+X(22)**2)/512
          T2=(X(61)**2+X(62)**2)/512
          T3=(X(101)**2+X(102)**2)/512
          T4=(X(141)**2+X(142)**2)/512
          T5=(X(181)**2+X(1822)**2)/512
          T6=(X(221)**2+X(222)**2)/512
          T7=(X(261)**2+X(262)**2)/512
C T8 IS NOISE ONLY.  COMPARE WITH THEORETICAL PFA
          T8=(X(301)**2+X(302)**2)/512
C COMPARE WITH THE ENERGY DETECTION THRESHOLD
          IF (T1.GT.ETA) P1=P1+1
          IF (T2.GT.ETA) P2=P2+1
          IF (T3.GT.ETA) P3=P3+1
          IF (T4.GT.ETA) P4=P4+1
          IF (T5.GT.ETA) P5=P5+1
          IF (T6.GT.ETA) P6=P6+1
          IF (T7.GT.ETA) P7=P7+1
          IF (T8.GT.ETA) P8=P8+1
10        CONTINUE
C OUTPUT THE SNR AND THE PROBABILITY OF DETECTION
        WRITE(*,*)FACTOR*0.001,0.0004*P1
        WRITE(*,*)FACTOR*0.002,0.0004*P2
        WRITE(*,*)FACTOR*0.003,0.0004*P3
        WRITE(*,*)FACTOR*0.004,0.0004*P4
        WRITE(*,*)FACTOR*0.005,0.0004*P5
        WRITE(*,*)FACTOR*0.006,0.0004*P6
        WRITE(*,*)FACTOR*0.008,0.0004*P7
        WRITE(*,*)0,0.0004*P8
C PREPARE FOR NEXT SIMULATION WITH DIFFERENT PFA
        P1=0
        P2=0
        P3=0
        P4=0
        P5=0
        P6=0
        P7=0
        P8=0
3     CONTINUE
      WRITE(*,*)
```

```
2       CONTINUE
        STOP
        END
```

XI. APPENDIX B: NCENT.FOR

```
C **  NCENT.FOR  ****************************************
C
C  FUNCTION     - PROBABILITY OF DETECTION FROM THE NON-
C                 CENTRAL CHI-SQUARE DIST EVALUATED AT THE
C                 SNR'S USED IN DETECT.FOR
C
C  PRECISION    - SINGLE
C
C  REQ'D ROUTINES
C               - BESSI0,QROMB NUMERICAL RECIPES
C
C  PROGRAMMER   - J. ERIC DUNN
C                 DEPT OF ELECTRICAL ENGINEERING
C                 IOWA STATE UNIVERSITY
C                 AMES, IOWA 50011
C                 (515)294-5174
C
C  LATEST REVISION  9/7/90
C ******************************************************
C
      EXTERNAL FOFQ

      COMMON RLAMBDA
      REAL X(63),N0
      DATA X/0.001,0.001778,0.002000,0.003,0.003162,
     & 0.003556,0.004000,0.004999,0.005334,0.005623,
     & 0.006000,0.006324,0.007113,0.008000,0.008891,
     & 0.009486,0.010000,0.010669,0.011246,0.012649,
     & 0.014226,0.015811,0.016870,0.017782,0.018973,
     &   0.020000,0.022493,0.025298,0.028117,0.030000,
     &   0.031622,0.033740,0.035565,0.040000,0.044987,
     &   0.049999,0.053348,0.056234,0.060000,0.063245,
     &   0.071131,0.080000,0.088913,0.094868,0.1,
     &   0.106696,0.112468,0.126491,0.142262,0.158113,
     &   0.168702,0.189736,0.2,0.224936,0.252982,
     &   0.281170,0.3,0.337404,0.4,0.449873,0.5,
     &   0.6,0.800000/

      WRITE(*,*)'PROBABILITY OF FALSE ALARM?'
      READ(*,*)PFA
C SINGLE SIDED NOISE SPECTRAL DENSITY.
      N0 = 0.50
C CALCULATE THE EERGY DETECTION THRESHOLD FOR A UNITY TIME
C BANDWIDTH PRODUCT RADIOMETER, NOISE VARIANCE IS 0.25,
C THE SINGLE-SIDED BANDWIDTH IS ASSUMED TO BE 1.
      ETA = -2.0 * LOG (PFA)
```

```
      DO 10 I=1,63
C BIN BANDWIDTH = 1 / 512
C TIME = 512 SECONDS
C TOTAL SIGNAL ENERGY IN THIS TIME:
        ES = 512*X(I)*X(I)/2
        RLAMBDA = 2 * ES / N0
C INTEGRATION OF NONCENTRAL CHI-SQUARE DISTRIBUTION W. 2
DEGREES
C OF FREEDOM USING ROUTINE FROM NUMERICAL RECIPES.
        CALL QROMB(FOFQ,ETA,100.,SS)
        WRITE(*,*)SS
10    CONTINUE
      STOP
      END

      REAL FUNCTION FOFQ(Q)
      COMMON RLAMBDA
      FOFQ = 0.5 * EXP(-0.5*(Q+RLAMBDA))*
     &                 BESSI0(SQRT(Q*RLAMBDA))
      RETURN
      END
```

XII. APPENDIX C: CLASSIM.FOR

```
C**** CLASSIM.FOR ***********************************************
C
C  FUNCTION        - TEST TWO PARAMETER CLASSIFIER.  THE FIRST
C                    PARAMETER HAS A GAUSSIAN DISTRIBUTION
C                    WITH KNOWN MEAN AND VARIANCE.  THE
C                    SECOND PARAMETER IS EMISSION FREQUENCY,
C                    WITH ORDER STATISTICS USED TO ESTIMATE
C                    THE HOPPING SPANS OF EACH FH SIGNAL.
C
C  PRECISION      - SINGLE
C
C  REQ'D ROUTINES- RAN1, GASDEV FROM NUMERICAL RECIPES
C                  FCOST
C
C  PROGRAMMER     - J. ERIC DUNN
C                   ELECTRICAL AND COMPUTER ENGINEERING
C                   IOWA STATE UNIVERSITY
C                   AMES, IOWA 50011
C                   (515)294-5174
C
C  LATEST REVISION - 10/02/90
C
****************************************************************
C
      PI = 3.14159265
      NTRIALS=100
      GDIST=1

C NUMBER OF OBSERVED EMISSIONS USED TO INITIALIZE THE HOPPING
C  SPAN ESTIMATES
      READ(99,*)NINIT
C CONSTANT FOR THE GAUSSIAN PDF'S.
      GCONST = 1.0 / SQRT (2 * PI)

C  D = NORMALIZED DISTANCE BETWEEN CENTER OF HOPPING SPANS
C       (SPAN WIDTH = 1)
      DO 10 D=0,2,0.1

C NTRIALS =THE NUMBER OF TIMES THE CLASSIFICATION ALGORITHM IS
C TESTED.
        DO 15 I=1,NTRIALS

C THE FIRST 100 EMISSIONS FROM EACH FH SIGNAL ARE GENERATED
C FOR EACH TRIAL
          DO 20 N=1,100
```

```
C X1,X2 = GAUSSIAN RV'S FROM FIRST AND SECOND FH SIGNALS
C         RESPECTIVELY.  2*GDIST STD DEVIATION SEPARATION
C         BETWEEN MEANS, P(ERROR)=0.159 FOR A SINGLE EMISSION
C         CLASSIFYER
            X1=GASDEV(IDUM)+GDIST
            X2=GASDEV(IDUM)-GDIST

C U1,U2 = UNIFORM RV'S REPRESENTING HOPPING FREQUENCY
            U1=RAN1(IDUM)+0.5*D
            U2=RAN1(IDUM)-0.5*D

            IF (N.EQ.1) THEN

C FIRST OBSERVATION.  INITIALIZE SPAN ESTIMATES.
C ND1,ND2 ARE THE NUMBER OF EMISSIONS (DWELL) OBSERVED FROM
C EACH FH SIGNAL
              ND1=NINIT
              ND2=NINIT
              A1=0.5*D
              B1=1+0.5*D
              A2=-0.5*D
              B2=1-0.5*D
C GENERATE HOPPING SAN ESTIMATES USING THE INVERSE CDF METHOD
              A1HAT = B1-(B1-A1)*(1.0 - RAN1(IDUM))**(1.0/ND1)
              B1HAT = A1+(B1-A1)*RAN1(IDUM)**(1.0/ND1)
              A2HAT = B2-(B2-A2)*(1.0 - RAN1(IDUM))**(1.0/ND2)
              B2HAT = A2 + (B2-A2) * RAN1(IDUM) ** (1.0 / ND2)
              A1=A1HAT
              B1=B1HAT
              A2=A2HAT
              B2=B2HAT
            ENDIF


C GCIJ = SIGNAL MATCH PROBABILITY FOR ASSIGNING R.V. FROM THE
C        I-TH PROCESS TO THE J-TH PROCESS USING GAUSSIAN DATA
            GC11= GCONST * EXP(-0.5*(X1-GDIST)**2)
            GC12= GCONST * EXP(-0.5*(X1+GDIST)**2)
            GC21= GCONST * EXP(-0.5*(X2-GDIST)**2)
            GC22= GCONST * EXP(-0.5*(X2+GDIST)**2)

C FCIJ = SIGNAL MATCH PROBABILITY USING EMISSION FREQUENCY
            CALL FCOST(FC11,FC12,U1,A1,A2,B1,B2,ND1,ND2)
            CALL FCOST(FC21,FC22,U2,A1,A2,B1,B2,ND1,ND2)

C TOTAL COST:
            C11 = GC11*FC11
            C12 = GC12*FC12
            C21 = GC21*FC21
```

```
            C22 = GC22*FC22
            T1 = C11 * C22
            T2 = C12 * C21

C TWO EMISSION CLASSIFICATION ALGORITHM
            IF (T1.GT.T2) THEN

C UPDATE ORDER STATISTICS BASED ON THE CLASSIFICATION DECISION
C THIS BRANCH REPRESENTS A CORRECT CLASSIFICATION DECISION
              A1 = MIN(A1,U1)
              B1 = MAX(B1,U1)
              ND1 = ND1+ 1
              A2 = MIN(A2,U2)
              B2 = MAX(B2,U2)
              ND2 = ND2 + 1
            ELSE

C THIS BRANCH REPRESENTS AN INCORRECT CLASSIFICATION DECISION
C TWO CLASSIFICATION ERRORS HAVE BEEN MADE
              A2 = MIN(A2,U1)
              B2 = MAX(B2,U1)
              ND2 = ND2 + 1
              PERR = PERR+1
              A1 = MIN(A1,U2)
              B1 = MAX(B1,U2)
              ND1 = ND1 + 1
              PERR = PERR+1
            ENDIF

20          CONTINUE
            TP = TP + PERR/(2*100)
            PERR = 0
15        CONTINUE

C OUTPUT THE RELATIVE DISTANCE BETWEEN PROCESS, AND THE
C AVERAGE PROBABILITY OF ERROR
          WRITE(15,*)TP/NTRIALS
          TP=0.0
10        CONTINUE
        STOP
        END

        SUBROUTINE FCOST(FC1,FC2,U,A1,A2,B1,B2,NH1,NH2)

        BC1=MAX(U,B1)
        AC1=MIN(U,A1)
        NE=NH1
        CBW = BC1 - AC1
```

```
P1 = NE*(NE-1)*((B1-A1)/CBW)**(NE-2)
P1 = P1 / CBW**3

BC2=MAX(U,B2)
AC2=MIN(U,A2)
NE=NH2
CBW = BC2 - AC2

P2 = NE*(NE-1)*((B2-A2)/CBW)**(NE-2)
P2 = P2 / CBW**3

TP = P1 + P2
FC1 = P1 / TP
FC2 = P2 / TP

RETURN
END
```